1 Calcification response of planktic foraminifera to environmental change in the
2 Western Mediterranean Sea during the industrial era

4 Thibauld M. Béjard[1*], Andrés S. Rigual-Hernández[1], José A. Flores[1], Javier P.
5 Tarruella[1], Xavier Durrieu de Madron[2], Isabel Cacho[3], Neghar Haghipour[4], Aidan
6 Hunter[5], Francisco J. Sierro[1]
7
8 1. Area de Paleontología, Departamento de Geología, Universidad de Salamanca,
9 37008 Salamanca, Spain
10 2. Université de Perpignan Via Domitia, CNRS, CEFREM, Perpignan, France
11 3. GRC Geociències Marines, Departament de Dinàmica de la Terra i de l'Oceà,
12 Facultat de Ciències de la Terra, Universitat de Barcelona, Barcelona, Spain
13 4. Earth Sciences Department, ETH Zurich, Zurich, 8092, Switzerland
14 5. British Antarctic Survey, Natural Environment Research Council, Cambridge,
15 United Kingdom
16
17 *Corresponding autor. E-mail address: thibauld.bejard@usal.es.

Abstract

18 Abstract
19
20 The Mediterranean Sea sustains a rich and fragile ecosystem currently threatened
21 by multiple anthropogenic impacts that include, among others, warming, pollution
22 and changes in seawater carbonate speciation associated to increasing uptake of
23 atmospheric CO_2. This environmental change represents a major risk for marine
24 calcifiers such as planktonic foraminifera, key components of pelagic Mediterranean
25 ecosystems and major exporters of calcium carbonate to the sea floor, thereby
26 playing a major role in the marine carbon cycle. In this study, we investigate the
27 response of planktic foraminifera calcification in the northwestern Mediterranean
28 Sea on different time scales across the industrial era. This study is based on data
29 from a 12-year-long sediment trap record retrieved in the in the Gulf of Lions and
30 seabed sediment samples from the Gulf of Lions and the promontory of Menorca.
31 Three different planktic foraminifera species were selected based on their different
32 ecology and abundance: *Globigerina bulloides*, *Neogloboquadrina incompta,* and
33 *Globorotalia truncatulinoides*. A total of 273 samples were weighted in both sediment
34 trap and seabed samples.
35 The results of our study suggest substantial different seasonal calcification patterns
36 across species: *G. bulloides* shows a slight calcification increase during the high
37 productivity period, while both *N. incompta* and *G. truncatulinoides* display a higher
38 calcification during the low productivity period. The comparison of these patterns

with environmental parameters indicate that controls on seasonal calcification are species-specific. Interannual analysis suggest that both *G. bulloides* and *N. incompta* did not significantly reduce their calcification between 1994 and 2005, while *G. truncatulinoides* exhibited a constant and pronounced increase in its calcification that translated in an increase of 20% of its shell weight. The comparison of these patterns with environmental data reveals that Optimum Growth Conditions affect positively and negatively *G. bulloides* and *G. truncatulinoides* calcification, respectively. Sea Surface Temperatures have a positive influence on *N. incompta* and *G. truncatulinoides* calcification, while carbonate system parameters appear to affect positively the calcification of three species in the Gulf of Lions throughout the 12-year time series.

Finally, comparison between sediment trap data and seabed sediments allowed us to assess the changes of planktic foraminifera calcification during the late Holocene, including the preindustrial era. Several lines of evidence indicate that selective dissolution did not bias the results in any of our data sets. Our results showed a weight reduction between pre-industrial and post-industrial Holocene and recent data, with *G. truncatulinoides* experiencing the largest weight loss (32-40%) followed by *N. incompta* (20-27%) and *G. bulloides* (18-24%). Overall, our results provide evidence of a decrease in planktic foraminifera calcification in the western Mediterranean, most likely associated with ongoing ocean acidification and regional SST trends, a feature consistent with previous observations in other settings of the world's oceans.

Key words: Planktic foraminifera, foraminifera calcification, biogeochemical cycles, Ocean Acidification, Mediterranean Sea.

1. Introduction

Growing population and its linked human activity since the industrial period (defined according to Sabine et al., (2004) from 1800 and therein) has caused an increase in carbon dioxide, which ecological and economic consequences are considered a major threat (Ipcc, 2022). Atmospheric CO_2 concentrations during the Pleistocene and Holocene ranged from 200 to 280 parts per million (ppm) (Loulergue et al., 2007; Lüthi et al., 2008; Parrenin et al., 2007), but these values have increased dramatically since the onset of the industrial period, exceeding the threshold of 400 ppm in 2015 for the first time for at least the last 800.000 years (Lüthi et al., 2008). This increase is significantly more important since the 1950s, when rapid atmospheric changes due to human activity took place, a process referred as "Great Acceleration" (Head et al., 2022a). Since then, between, 25 and 30% of

77 anthropogenic CO_2 has been absorbed by the world's ocean (Sabine et al., 2004).
78 The ocean uptake of atmospheric CO_2 causes a drop in both pH and carbonate ion
79 concentration (Barker et al., 2012), lowering seawater alkalinity; this process is
80 commonly known as Ocean Acidification (OA), and it is expected to affect all areas
81 of the ocean and to have a wide impact on marine life (Davis et al., 2017; Figuerola
82 et al., 2021; Orr et al., 2005). One of the main questions about recent environmental
83 change is how different ecosystems and regions in global ocean are going to react
84 to the ongoing increase of anthropogenic atmospheric carbon dioxide.
85 A large body of evidence indicates that ocean acidification has substantial and
86 diverse effects on the distribution and fitness of a wide range of marine organisms
87 (Kroeker et al., 2013; Meier et al., 2014; Moy et al., 2009). For example, some fleshy
88 algae and diatom species have been shown to increase their growth and
89 photosynthetic activity at enhanced CO_2 concentrations (Kroeker et al., 2013). In
90 turn, most calcifying organisms such as calcifying algae, corals, pteropods,
91 coccolithophores and foraminifera are negatively affected by this process often
92 showing a reduction in their abundance, calcification and growth rates (Kroeker et
93 al., 2013; Orr et al., 2005).
94 Planktic foraminifera are a group of marine single-celled protozoans that produce
95 calcareous shells. Their distribution across the water column is conditioned by
96 factors that include, but are not limited to, food availability, temperature, salinity and
97 sunlight (Schiebel and Hemleben, 2005). These organisms are considered to play a
98 key role in marine carbon cycle and carbonate production, accounting for between
99 32 and 80% of the deep ocean calcite fluxes (Schiebel, 2002). Depending on their
100 ecology and feeding strategies, these organisms can be algal (dinoflagellates)
101 symbiont bearing or not symbiont bearing and be spinose or non-spinose. Planktic
102 foraminifera represent a useful tool for palaeoecological and palaeoceanographic
103 studies, as the abundances of different species and their geochemical signature
104 allow reconstructing sea surface temperatures and water column physical and
105 chemical properties (Lirer et al., 2014; Margaritelli, 2020; Schiebel and Hemleben,
106 2017).
107 Previous studies suggest that planktic foraminifera are sensitive to ocean
108 acidification (OA). Laboratory experiments indicate that when carbonate ion
109 concentration decreases, shell weight and calcification decrease too in a variety of
110 species (Bijma et al., 2002; Lombard et al., 2011). Species that host symbionts have
111 been described showing a higher tolerance to dissolution due to the capacity of algal
112 symbionts to alter immediate seawater chemistry (Lombard et al., 2009). Moy et al.
113 (2009) documented a decrease of 30-35% shell weight in the planktic foraminifera
114 *G. bulloides* during the industrial era in the subantarctic Southern Ocean, most likely
115 induced by anthropogenic-driven ocean acidification. A recent study by Fox et al.

116 (2020) showed that non-spinose (*N. dutertrei*) foraminifera species exhibit a more
117 pronounced calcification reduction than the spinose (*G. ruber*) species in response
118 to increasing CO_2. The main difficulty for studying the impact of OA on foraminifera
119 (and any calcifying organisms) resides in finding long-term continuous records in
120 order to be able to evaluate possible changes in shell calcification (Fox et al., 2020).
121 In order to assess the impact of recent environmental change on planktic
122 foraminifera, in this work we present data from Planier sediment trap (data from 1993
123 to 2006) (Rigual-Hernández et al., 2012) and from seabed sediments from three
124 different sites located in both the Gulf of Lions and the promontory of Menorca. The
125 Mediterranean Sea is a semi-enclosed sea with a high saturation state for calcite
126 (Álvarez et al., 2014). It is often considered as a "miniature ocean" and a "laboratory
127 basin" (Bergamasco and Malanotte-Rizzoli, 2010) which makes it a valuable zone to
128 study the response of marine calcifying organisms to environmental change.
129 The advantage of sediment traps is that they can provide data coming from annual
130 fluxes, avoiding the effects of seasonal abundance and ontogeny and making
131 interannual comparisons more reliable (Jonkers et al., 2019). Three different planktic
132 foraminifera species, each of which characterized by contrastingly different depth
133 habitats and ecologies, were selected for our analysis: *G. bulloides,* a spinose
134 opportunist surface dweller that lies above the thermocline (Schiebel and Hemleben,
135 2014); *N. incompta,* a non-spinose temperate surface dweller; and *G.
136 truncatulinoides,* a non-spinose deep dwelling species which migrates through the
137 water column with a complex life cycle. Our aims for this study are: (i) to compare
138 two widely used foraminifera weighing and size-normalization techniques and
139 provide a baseline of modern foraminifera weight data and calcification in the
140 Western Mediterranean against which future changes in foraminifera calcification
141 can be assessed (ii) document seasonal and interannual trends in the planktic
142 foraminifera calcification of the three planktic foraminifera species, and (iii) evaluate
143 possible changes in shell calcification through the Holocene to the present day by
144 comparing shell weights of the foraminifera collected by the traps with those of the
145 seafloor sediments.

2. Study area

148 The Mediterranean is a semi-enclosed sea and is considered a concentration basin
149 (Bethoux et al., 1999) with a negative hydrological budget: fresh water inputs do not
150 compensate the overall basin evaporation. The surface oceanic waters that enter
151 the Mediterranean through the Strait of Gibraltar and spread towards the eastern
152 basin compensate this negative balance. The waters of Atlantic origin (AW) circulate
153 according to a cyclonic circuit (counterclockwise) along the Mediterranean rim (Fig.

154 1a). In the northwestern basin, this along-slope current, called the northern current
155 (NC), is formed by the convergence at the level of the Ligurian Sea (LS) of the waters
156 flowing on both sides of Corsica. The general circulation in this sub-basin forms a
157 cyclonic pattern, flowing westward along the Gulf of Lions, bypassing the Balearic
158 Sea and finally closing its circuit eastward along the North Balearic Front (NBF) (Fig.
159 1b).

160
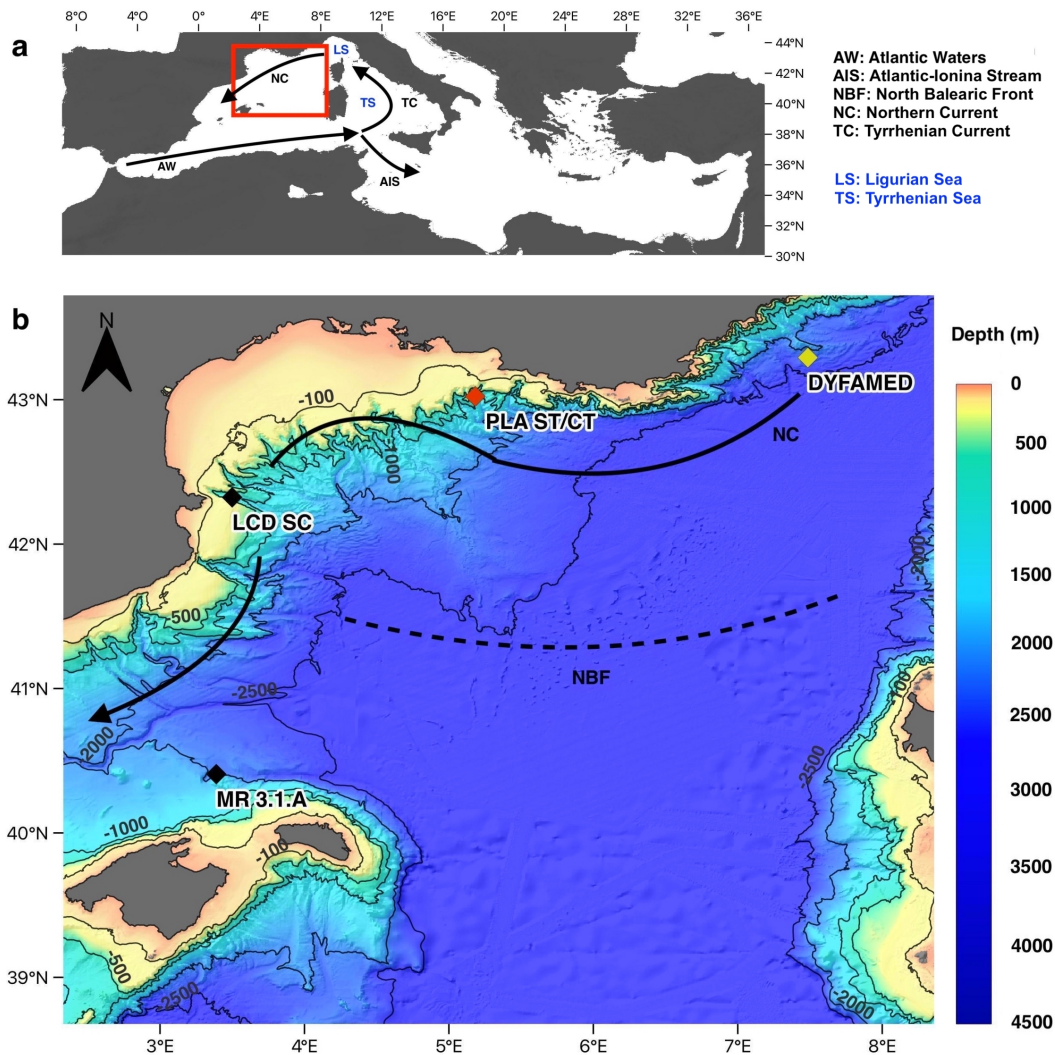
161 **Figure 1. a.** Study area location in the Mediterranean Sea and general
162 surface circulation **b.** geographic setting of the Gulf of Lions and location of
163 studied sites. Red diamond shows the position of the Planier site sediment
164 trap and core-top (PLA ST/CT). Black diamonds represent the location of the
165 seabed sediments samples analyzed from Lacaze Duthiers canyon (LCD SC)
166 and Menorca promontory (MR 3.1A). Yellow diamond represents the location
167 of the Dynamics of Atmospheric Fluxes in the MEDiterranean Sea
168 (DYFAMED) site, located 200 km upstream Planier station position. Arrows

169   represent the surface circulation (Millot, 1999). The topographic model was
170   downloaded from the GEBCO database.

171 Moreover, the Mediterranean is recognized as a sensitive region to increasing
172 atmospheric CO_2 (Ziveri, 2012) due to the fast turnover time of its waters (Béthoux
173 et al., 2005) and the fast penetration of anthropogenic CO_2 (Schneider et al., 2007).
174 Sea surface temperatures are predicted to increase by 1.5-2°C by the end of the
175 century, a faster rate than the global average (Lazzari et al., 2014). pH is expected
176 to decrease according to the global average (0.3-0.4 units by 2100) or even exceed
177 the global trend (Hassoun et al., 2015). The Mediterranean Sea is also affected by
178 other stressors, which impact marine organisms in many ways (Lejeusne et al.,
179 2009). Finally, it is also a region shaped by human development and its associated
180 activities interact with environmental changes (Mediterranean Experts on Climate
181 Change, MedECC, 2019).
182 The Gulf of Lions is located in the northwestern part of the Mediterranean Sea, and
183 its morphology presents a continental slope with an array of complex submarine
184 canyons (Rigual-Hernández et al., 2012) (Fig. 1b). Vertical mixing, generated by
185 intense surface cooling and evaporation, occurs in winter in the Gulf of Lions driven
186 by cold, dry northern winds, resulting in dense water on the shelf and offshore
187 (Durrieu de Madron et al., 2005; Houpert et al., 2016; Millot, 1990). This winter mixing
188 recharges surface waters with nutrients. This enrichment with increased solar
189 radiation stimulates primary production in spring. Increasing heat fluxes during
190 spring and summer cause water mass stratification and nutrient depletion, which
191 lasts until late summer, until fall cooling breaks the stratification of the water column
192 and causes a fall bloom (Heussner et al., 2006; Monaco et al., 1999; Rigual-
193 Hernández et al., 2012). River inputs are the main source of suspended particles in
194 the Gulf of Lions, and the Rhone river represents the most important river in the
195 northwestern Mediterranean; however, other sources include Saharan dust deposits
196 and biological production (Heussner et al., 2006; Monaco et al., 1999). Overall, the
197 oceanographic setting of the Gulf of Lions is an exception to the general oligotrophy
198 of the Mediterranean Sea.

199   3. Material and methods
200
201   **3.1.   Sediment traps, core-tops and sediment cores.**
202 A series of deployments of sediment traps mooring lines in the Gulf of Lions
203 continental margin was initiated in 1993 within the framework of several French and
204 European projects (PNEC, Euromarge-NB, MTP II-MATER, EUROSTRATAFORM)
205 and the monitoring of two sites, Planier and Lacaze-Duthiers stations (Fig. 1),
206 continues as a component of the MOOSE program (Mediterranean Ocean

207 Observing System for the Environment) (Coppola et al., 2019). Planier station
208 (43°02'N, 5°18'E) is located at the northeastern end of the Gulf of Lions, in the axis
209 of the Planier Canyon. The sediment trap used for this work was located at around
210 530 m water depth in a water column of ~1000m. Further details of the mooring
211 design can be found in Heussner et al., (2006). Planktic foraminifera fluxes for the
212 1993 to 2006 period were documented by Rigual-Hernández et al., (2012). Here, we
213 used the samples from the latter study for our weight and calcification analysis. This
214 sediment trap is used here as a baseline of the planktic foraminifera dwelling in the
215 modern Mediterranean Sea. Moreover, we analyzed a set of core top and sediment
216 cores collected from several locations of the Northwestern Mediterranean that are
217 considered to represent foraminifera assemblages sedimented during the Holocene
218 era (Table 1).

219   **Table 1**. Description of the core tops used in this study. Data for Planier core-
220   top (PLA CT) and Lacaze-Duthiers sediment core (LCD SC) are available in
221   Heussner et al., (2006), and data concerning Menorca sediment core (MR
222   3.1.A) can be found in Cisneros et al., (2016). Conventional ^{14}C ages, 1-sigma
223   uncertainties, local reservoir and the calibrated age have been rounded
224   according to convention. See section 3.7 for details concerning "Bomb [14]C".

Site	Location	Water depth (m)	Sediment Samples	Samples Depth (cm)	Sample dated	Species dated	Radiocarbon age (^{14}C years BP)	1-sigma error (^{14}C years)	Local reservoir (^{14}C years BP)	Calibrated age (cal. years BP)
PLA CT	42.989° N 5.121° E	1095	2	0-1	0.5-1 cm	*G. bulloides*	490	60	165 ± 95	Bomb [14]C
LCD SC	42.265°N 3.54°E	990	7	0-5	0.5-1 cm	*G. bulloides*	460	60	165 ± 95	Bomb [14]C
MR 3.1.A	40.29°N 3.37° E	2117	40	0-27	14-14.5 cm	*G. bulloides*	1980	65	165 ± 95	1560

225

226 ## 3.2. Sediment core samples processing

227 A total of 2 sediment samples from Planier core top, 7 from Lacaze-Duthiers
228 sediment core and 40 from Minorca sediment core were weighed (Table 1). Dry bulk
229 sediment samples from all sites was weighed using a Sartorius CP124S balance
230 (precision= 0.1mg).
231 The samples were then wet-sieved in order to separate the <63 μm fraction and dry
232 sieved to separate the bigger fractions (>150 μm and >300 μm). The sediment
233 washing was carried out with potassium phosphate-buffered solution (pH= 7.5) in
234 order to optimize foraminifera preservation. Each fraction was oven dried at a
235 constant temperature (50°C) and then weighed. The >150 μm fraction was used for
236 identification, counting and shell morphometric and weight analyses.

237

3.3. Ecology and life cycle of *Globigerina bulloides*, *Neogloboquadrina incompta* and *Globorotalia truncatulinoides*

G. bulloides is a spinose surface to sub-surface dweller (Schiebel and Hemleben, 2017a), found in the upper 60 m of the water column. This species has affinity for temperate to sub-polar waters and upwelling systems in lower to mid latitudes (Azibeiro et al., 2023; Bé et al., 1977). In terms of its seasonal distribution, it has been documented to be associated to enhanced productivity periods in mid to high latitudes (Chapman, 2010; Schiebel and Hemleben, 2005). No symbiont algae are hosted by this species and, contrary to most spinose species, its diet is mainly algae based (Schiebel et al., 2001). *G. bulloides* shows an opportunistic feeding and strategy, leading to a high abundance in the foraminifera assemblages preserved in the sedimentary record. This is despite its tests have been documented to be more susceptible to dissolution than the average of the planktic foraminifera species (Dittert et al., 1999).

N. incompta is a surface dweller abundant in subpolar to temperate water masses across all the ocean basins (Kuroyanagi and Kawahata, 2004). This is a non-spinose species and does not carry symbiont algae. In North-Atlantic waters, *N. incompta* is a major component of foraminifera assemblages from late spring to late fall, and generally, is the dominant foraminifera species during late summer when maximum shoaling of mixed layer depths occur (Schiebel and Hemleben, 2000). It shows a minor presence in low latitudes and during periods of enhanced nutrient supply, *N. incompta* is outnumbered by other more opportunistic species, (Schiebel et al., 2002).

G. truncatulinoides is considered the deepest dweller among the extant planktic foraminifera, with living specimens documented below 2000 m (Schiebel and Hemleben, 2005). Considered a widespread species, it can be found from subpolar to subtropical water masses (Schiebel and Hemleben, 2017). It is a non-spinose species (Margaritelli, 2020), and it does not carry any symbiont algae (Takagi et al., 2019). An important aspect to highlight about this species is its complex life cycle (Margaritelli et al., 2022). It reproduces once a year in the upper water column during late winter, when mixing of the water column allowed the migration of juveniles to the surface waters (Lohmann and Schweitzer, 1990; Schiebel et al., 2002). The former authors speculated that nutrient availability and the avoidance strategies to predation could explain this its life cycle. Then, the adult migrate downward the water column (Rebotim et al., 2017) and spend the rest of their life cycle developing an additional calcite layer in cooler waters below the thermocline (Lohmann and Schweitzer, 1990; Wilke et al., 2009). Around 70% of *G. truncatulinoides* calcification

275 has been estimated to take place around the thermocline, while the remaining 30%
276 take place in surface waters (LeGrande et al., 2004).
277 The abundance of these three species has been previously studied in the Gulf of
278 Lions by Rigual-Hernández et al., (2012). The latter study showed that both *G.*
279 *bulloides* and *N. incompta* displayed their maximum abundances during the spring
280 bloom, while *G. truncatulinoides* abundance was maximum during early winter. On
281 the other hand, minimum abundances were reached during late spring and summer
282 for *G. bulloides* and *N. incompta* respectively, and *G. truncatulinoides* displayed a
283 minimum abundance during fall.
284
285 ### 3.4. Foraminifera picking and mass and size estimations
286 Different sizes were selected depending on the maximum availability of each
287 species: 250-300, 200-250 and 400-500 µm for *G. bulloides, N. incompta* and *G.*
288 *truncatulinoides*, respectively. For the latter species, both coiling morphotypes were
289 selected although the right coiling was substantially less abundant representing less
290 than 3% in our counts, a feature consistent with the literature that indicates a low
291 presence of right coiled specimens (Margaritelli et al., 2020; 2022).
292 A total of 273 foraminifera samples were picked for this study, 126 coming from the
293 sediment trap and 147 from the three sediment cores and core tops (Table 2).
294 However, these numbers represent the total of samples analyzed but unique
295 samples number is lower, as not all the sediment trap samples presented the three
296 species in high enough numbers to perform the picking. The species were analyzed
297 in size fractions in order to estimate the efficiency of sieve fractions and the impact
298 of size and morphometric parameters on the foraminifera weight and calcification.
299 The mean weight of each available sediment trap sample was obtained by weighting
300 between 15 to 45 specimens of *G. bulloides* (mean N= 27), 5 to 25 *N. incompta*
301 (mean N= 15) and 5 to 25 *G. truncatulinoides* (mean N= 13). Concerning the
302 analyses of the core top and sediment core samples, between 15 and 25 *G. bulloides*
303 and *N. incompta* (mean N= 20 for both) and between 9 and 25 *G. truncatulinoides*
304 (mean N= 18) were picked.
305 Each foraminifera sample was then cleaned by gentle ultrasonication (50 Hz) for 5
306 to 75 seconds (depending on the species and the degree of visual uncleanliness) in
307 methanol in order to clean the shells. The samples were then left to dry in a
308 temperature-controlled oven at 50°C. One out of three analyzed samples were
309 weighted before and after cleaning in order to assess potential shell mass losses
310 and shell preservation due to ultrasonication. Our results indicate that this method
311 has little impact on shell preservation with around 95% of the total foraminifera
312 conserved in good conditions. Weight loss between non-cleaned samples and
313 cleaned samples is a mean 0.5 to 3 µg (between 6 and 32% of the sample total

314   measured weight) depending on the species, mainly due to the presence of clay and
315   non-calcite material in the shells, which justifies this cleaning process (see
316   Supplementary fig. 6).
317   The weightings were carried in the micropaleontology laboratory of the Geology
318   Department at University of Salamanca using a Sartorius ME5 balance (precision=
319   0.001 mg). This method allowed us to obtain foraminifera Sieve Based Weight
320   (SBW) by dividing the average shell weight per sample (5-45 tests) by the total
321   number of foraminifera within each sample. The lowest number of individuals
322   selected per sample was five in order to maximize the number of samples available
323   for our study. According to Beer et al., (2010), the higher the number of individuals,
324   the more reliable SBWs are. Here we aim to compare SBW results with a measured
325   weight technique. Measured techniques are acknowledged to be reliable with a lower
326   number of individuals, therefore a minimum of five individuals were selected in order
327   to compare the two techniques.
328   However, it has been described that traditionally used sieve fractions method is
329   considered unreliable because of the effect of morphometric parameters on the
330   foraminifera weight (Beer et al., 2010). In order to remove the size effect on the
331   weight, the mean SBW was normalized to the mean diameter and area of the
332   planktic foraminifera to obtain Measurement Based Weights (MBW). Morphometric
333   parameters were measured using a Nikon SMZ18 stereomicroscope equipped with
334   a Nikon DS-Fi3 camera and NISElements software. These measurements were
335   carried out on the same shells that were weighted. Foraminifera shells were
336   positioned in order to obtain the maximum area of each individual, in this case, the
337   umbilical side (aperture facing upwards) was measured for the three species.
338   MBW_{area} and $MBW_{diameter}$ were calculated according to the following formula
339   (Aldridge et al., 2012; Beer et al., 2010), where "parameter" accounts for "area" or
340   "diameter":
341
342   $$MBW\,sample = \frac{mean\ SBW_{sample} \times mean\ parameter_{size\ fraction}}{mean\ parameter_{sample}}$$
343
344   "Size fraction" accounts for the mean of the parameter (area or diameter) measured
345   in all the sites studied, while "sample" accounts for the mean of the parameter in the
346   particular sample being measured. The advantage of these measurements is that
347   the resulting MBW is being given with a weight unity (μg), thereby allowing direct
348   comparison with other studies (Beer et al., 2010) and useful for estimating their
349   contributions to marine biogeochemical cycles.
350   Correlations between SBW and MBW_{area} against area are displayed in Fig. 2. The
351   reason for this comparison is to show the relation between size and weight and to

352 avoid the effect of having the bigger specimens displaying the heaviest weight and
353 impacting the mean weight (therefore calcification indicator) of the sample.
354 Finally, in order to compare weights patterns from the sediment trap with weights
355 from core tops and sediment cores and overcome the seasonality effect, MBWs were
356 flux-weighted. Mean monthly MBWs values from each species were multiplied by
357 the corresponding mean monthly flux and then divided by the total annual flux of the
358 corresponding species. For these calculations, the flux data from each species
359 estimated for the >150 μm fraction from Rigual-Hernández et al., (2012) was
360 employed.
361
362 ### 3.5.   Environmental data
363 Foraminifera fluxes and abundances together with chlorophyll-a were taken from
364 Rigual-Hernández et al., (2012) for the entire time span of the analyzed samples.
365 Both fluxes and abundance come from direct sediment observation from the Planier
366 site, while chlorophyll-*a* data was obtained from SeaWiFS monthly measurements
367 through NASA's Giovanni program on a 0.2 x 0.2° area around the mooring location.
368 SeaWiFS measurements started in 1997 and were used due to the lack of direct
369 chlorophyll measurements in our samples. Sea Surface Temperature (SST) was
370 recovered from the NOAA database with the same gridding as the data from the
371 NASA's Giovanni program.
372 Salinity, nutrient concentrations (nitrates and phosphates) and carbonate system
373 parameters data were collected from the DYFAMED database (http://www.obs-
374 vlfr.fr/dyfBase/index.php) (Coppola et al., 2008; 2021). DYFAMED site is located
375 around 200-220 km (Fig. 1b) east of the sediment trap location (43°25´N, 7°52´E), in
376 the Ligurian Sea. From an oceanographic view, its situation is upstream of the NC
377 circulation and can be considered representative of seasonal and interannual
378 variability of biological and water column properties of the open-ocean waters in the
379 northwestern Mediterranean (Heussner et al., 2006; Meier et al., 2014). Alkalinity
380 and total carbon measurements were available for years 1998 to 2000 and mid 2003
381 to 2005. Missing values comprised in these years were replaced with values
382 obtained from linear regression of the measurements from above and below. The
383 CO2SYS macro has been used to reconstruct the $[CO_2]$, $[CO_3^{2-}]$, $[HCO_3^-]$ and pH
384 values from the measured total alkalinity and dissolved inorganic carbon. The
385 constants used were the CO_2 dissociation constant by Mehrbach et al., (1973) refit
386 by Dickson and Millero, (1987); the $KHSO_4$ by Dickson, (1990); and the seawater
387 scale for pH.
388
389 ### 3.6.   Statistical analysis

390 In order to have uninterrupted monthly environmental values from the DYFAMED
391 site during available measurements, a resampling every 10 days has been carried
392 out with the QAnalySeries program.
393 Independence and correlation between the area the different species SBWs and
394 MBW$_{area}$ was tested using a Pearson linear correlation test with an R script (see
395 Supplementary material).
396 Seasonal correlation analyses were carried out with the Statistica program. A $p<0.05$
397 was used in order to consider a correlation as significant. The number (N) of
398 correlations depended on data availability and was 10 for *G. bulloides*, 9 for *N.*
399 *incompta* and 12 for *G. truncatulinoides*.
400 It should be noted that the analysis of interannual trends was hindered by gaps in
401 the sediment trap record and by the low number of specimens during some sampling
402 intervals. Therefore, interannual trends in planktonic foraminifera calcification should
403 be interpreted with caution.
404 The influence of environmental variables upon MBW$_{area}$ was assessed using
405 General Additive Models (GAM) (fitted using the *gam* function from the *mgcv* R
406 package). Due to data limitation, the GAMs could not be fitted to multiple
407 independent variables, so potential effects of interacting environmental variables
408 were could not be assessed. Each model tested the dependence of the different
409 MBW upon a single independent variable: month or year, to evaluate seasonal and
410 interannual trends; the flux of each species, to test effects of ecological variability;
411 and a suite of environmental variables to determine impacts of various aspects of
412 ocean chemistry on the calcification. Smooth functions of these measured quantities
413 were used as the single independent variable within the GAMs, which were fitted
414 using the default settings of the *gam* function: a Gaussian family and identity link
415 function; and the GCV.cp smoothing method. GAM results quantified the
416 significance of the effect of each independent variable upon MBW.
417 In order to investigate the difference between the MBW data from the sediment trap
418 and the core-top /sediment cores, a non-parametric two-way Mann-Whitney test has
419 been performed. This test determines if there are significant differences in the
420 medians of data sets without making assumptions about the data distributions. A p-
421 value <0.05 has been used to consider the median of two datasets different.
422
423 ### 3.7.   Radiocarbon dating
424 Between 50-100 individuals of well-preserved *G. bulloides* shells (>150 μm) were
425 picked for radiocarbon analyses. Radiocarbon ($^{14}C/^{12}C$) was measured as CO_2 with
426 a gas ion source in a Mini Carbon Dating System (MICADAS) at the Laboratory of
427 Ion Beam Physics from ETH Zürich. The employed automated method consists of
428 initial leaching of the outer shell to remove surface material with 100 μl of ultrapure

429   HCl (0.02M) and the subsequent acid digestion of the remaining carbonates with
430   100 μl of ultrapure H_3PO_4 (85%) (Wacker et al., 2013). Therefore, no cleaning was
431   applied after the picking contrary to the samples used for mass and size
432   measurements. Marble (IAEA-C1) was used for blank correction and results were
433   corrected for isotopic fractionation via $^{13}C/^{12}C$ isotopic ratios.
434   Conventional radiocarbon age for sample 14-14.5cm from MR 3.1.A site was
435   calibrated with the on-line calibration program CALIB (Stuiver and Reimer, 1993)
436   using the Marine20 curve, which applied a marine reservoir correction of 550 ^{14}C
437   years (Heaton et al., 2020) to the corresponding ^{14}C age and error. Additionally, a
438   local reservoir effect (Stuiver and Braziunas, 1993) of -165 ± 95 ^{14}C years was
439   considered. This local reservoir was calculated as the average of the 8 nearest
440   points to the sample location from the Marine Reservoir Correction database
441   (Reimer and Reimer, 2001), whose values have already been corrected for the
442   Marine20 curve. ^{14}C ages from samples 0.5-1cm from both PLA CT and LCD SC
443   lied out of the range for calendar calibration, implying these samples contain some
444   bomb ^{14}C and cannot be considered pre-industrial (Table 1, see "bomb ^{14}C"). In order
445   to have an estimation of the time span that could be covered by these dates, the
446   same marine and local reservoir corrections were applied to the most recent ^{14}C date
447   that could be corrected (i.e. 603 ^{14}C years BP). As the $F^{14}C$ for this sample was <1
448   (see Supplementary table 1), this means that the ^{14}C found in these samples is not
449   dominated by the bomb carbon. Here we propose a 110-50 cal. years BP age for
450   these samples. Then, these samples could be considered post-industrial. The
451   detailed results of the calibration and the ^{14}C dating can be found in the
452   Supplementary figs. 1 and 2.
453   Finally, it is important to consider that these ^{14}C ages represent mean average
454   values. Therefore, time integration within each sample and the effects of bioturbation
455   could cause a variation on the foraminifera real ages (Dolman et al., 2021).
456   Both the samples and dates obtained are detailed in Table 1. Planktic foraminifera
457   present in the dated samples that were not selected for radiocarbon dating were also
458   analyzed following the methodology described previously.

459   ## 4. Results
460

461   **4.1. Shell morphometric parameters and shell-weight normalization**

462   **Table 2**. Minimum, mean, maximum and standard deviation values of shell
463   area, diameter and SBW for *G. bulloides, N. incompta* and *G. truncatulinoides*
464   at all studied sites. The last 3 columns show the number of samples, the mean
465   number (N) of individuals analyzed per sample and the total number of
466   individuals measured for each site.

	Area (µm²)				Diameter (µm)				Sieve Based Weight (SBW, µg)				Total samples	N per sample	total N
PLA Sediment Trap	Min	Mean	Max	Std.Dev	Min	Mean	Max	Std.Dev	Min	Mean	Max	Std.Dev			
G. bulloides	16978	57353	168492	17261	147.0	267.5	463.2	38.6	3.21	4.43	5.60	0.66	35	27.2	893
N. incompta	26234	42821	135422	8934	182.8	232.4	415.2	22.6	3.17	4.45	5.40	0.59	32	15.0	455
G. truncatulinoides	70712	178952	527622	63572	291.9	468.5	819.6	81.9	10.67	23.11	39.57	7.79	59	13.0	729
PLA Core-Top															
G. bulloides	37163	55395	87894	12302	217.5	264.0	334.5	28.8	5.00	5.22	5.43	0.30	2	17.3	39
N. incompta	27635	36927	49619	5447	187.6	216.3	251.4	15.9	4.46	4.46	4.46	0.00	2	19.7	41
G. truncatulinoides	89778	174748	233229	44313	338.1	467.7	544.9	61.9	34.80	35.40	35.90	0.70	2	14.7	34
MIN Sediment core															
G. bulloides	20895	52132	138424	8722	163.1	256.8	419.8	20.5	4.00	5.07	6.57	0.46	40	19.6	761
N. incompta	24003	35098	57264	4658	174.8	211.0	270.0	13.7	3.45	4.11	5.00	0.34	40	20.3	791
G. truncatulinoides	116686	166318	365851	23262	385.4	459.1	682.5	30.8	28.33	34.99	42.60	3.25	40	14.4	576
LCD Sediment core															
G. bulloides	27624	52472	116605	8793	187.5	257.7	385.3	20.4	4.35	4.73	5.19	0.31	7	20.1	136
N. incompta	28089	37789	51284	4972	189.1	218.9	255.5	14.4	3.68	4.12	4.50	0.26	7	19.8	134
G. truncatulinoides	82534	143138	393754	41620	324.2	423.3	708.1	55.9	25.27	26.68	30.66	1.94	7	15.3	105

467

468 Overall, the mean values for both diameter and area correspond to the mean
469 narrowed size fraction used during the picking, but morphometric parameters show
470 some variability between the studied sites. Standard deviation of both area and
471 diameter values for the three species are higher in the sediment trap record than in
472 seafloor sediments, with mean values (of all three species) of 82% higher for area
473 and 69% higher for diameter. SBW exhibits the same pattern as both area and
474 diameter standard deviation is a mean 130% higher in the Planier sediment trap.
475 Regarding the variability across the seafloor samples, Planier core-top exhibits a
476 greater area and diameter values (about 40 to 50% increase for the three species)
477 compared to those of the other two sediment cores, probably due to the fewer
478 samples analyzed (Table 2).
479 The Planier sediment trap results (Table 2) show a higher standard deviation for both
480 area and diameter for the three species, i.e. 76 % and 68% higher for *G. bulloides*
481 compared to the data from core tops, 78% and 54% for *N. incompta* and 81% and
482 73% for *G. truncatulinoides*.
483 Because of the lack of precision of the initial individuals picking, carried out with a
484 micrometer installed in the microscope, the selection is not totally accurate. Due to
485 this issue, one third of the of the total measured foraminifera (i.e. 1645 of 4694) were
486 out of the desired size fraction, of which 12% were bigger (580/4694) and 23% were
487 smaller (1065/4694). Nonetheless, only 0.02% were more than 20% out of the
488 selected size range (64/4694 more than 20% bigger and 29/4694 more than 20%
489 smaller). Mean size difference for the foraminifera out of the size fraction is around
490 7%. Results vary according to the site and the species. 50% of the individuals from

491   the Planier sediment trap (1046/2077) and 26% of the individuals coming from the
492   core tops (692/2617) were out of range. *G. bulloides* showed a 45.5% (53.2% in the
493   sediment trap and 39.3% in the core-tops samples) of individuals out of selected size
494   fraction, while this value was 21.5% (22.2% in sediment trap, 21.1% in sediment
495   cores) for *N. incompta* and 35% for *G. truncatulinoides* (53.4% in sediment trap,
496   16.7% in sediment cores).
497   Even though a narrow size class was selected for each species (see section 3.4), a
498   clear influence of the area on the SBW was found in our data set (Fig. 2).
499
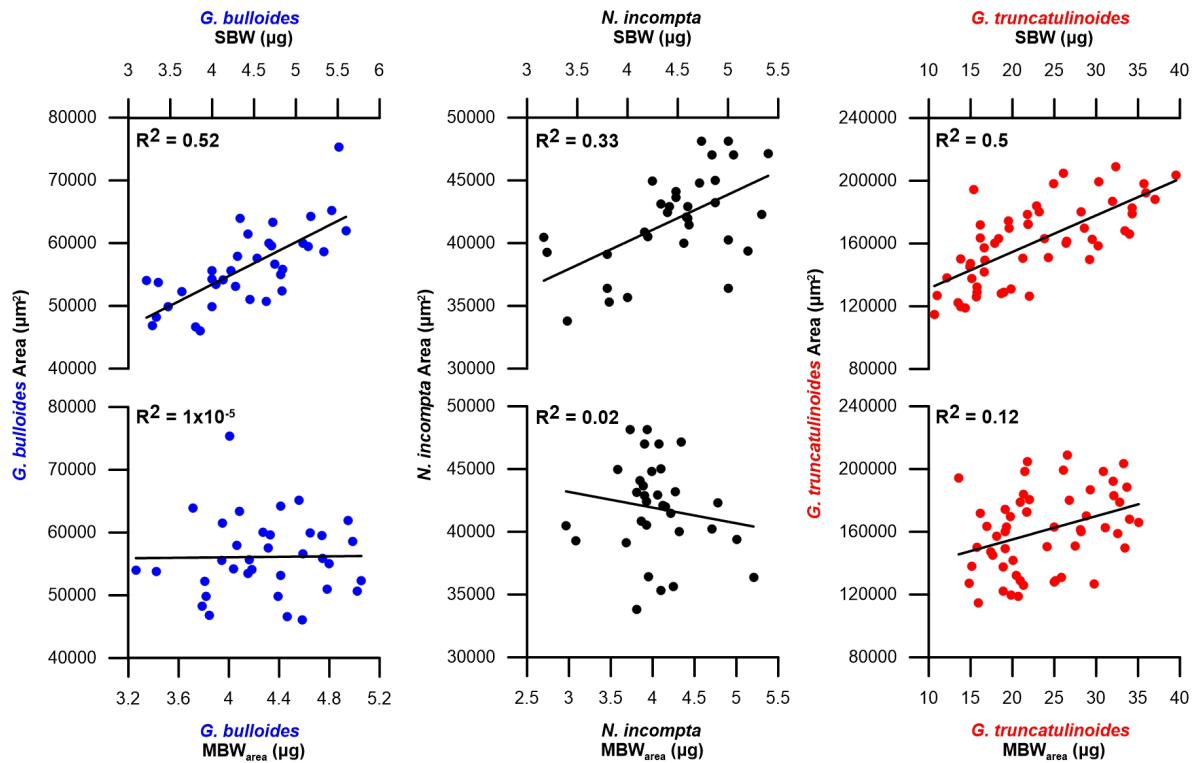
501   **Figure 2**. SBW in μg and MBW$_{area}$ in μg against the mean test area in μm^2 for
502   foraminifera samples in the Planier sediment trap. Dark blue dots correspond
503   to *G. bulloides*, black dots to *N. incompta* and red dots to *G. truncatulinoides*.

504   In particular, SBW shows a positive correlation with area: $0.33 < r^2 < 0.53$ (Fig. 2). This
505   indicates that the SBW is dependent on the size of the specimens within the selected
506   size range. Thus, to isolate the component of variation in foraminifera shell thickness
507   that represents a change in calcification and does not occur as a direct result of
508   changes in shell size, normalization of the shell weight was performed following the
509   formula detailed in section 3.3. (Beer et al., 2010). After normalization MBW$_{area}$
510   shows no correlations with area: $1 \times 10^{-5} < r^2 < 0.12$ (Fig. 2). Note that the weight
511   variations in our dataset are quite considerable, especially for *G. truncatulinoides*,
512   probably due to the wider size fraction. Diameter does show correlation with SBW:

513     $0.33<r^2<0.5$; and shows a non-negligible correlation with MBW_{diam}: $0.2< r^2 <033$. Our
514   data demonstrates that SBW correlates more strongly with MBW_{diam} than with
515   MBW_{area} for the 3 species: 0.9>0.48 for *G. bulloides*, 0.89>0.52 for *N. incompta* and
516   0.97>0.81 for *G. truncatulinoides*. These values are consistent with previous studies
517   (Beer et al., 2010).

518   **Table 3.** Pearson correlation test results for the three species correlation
519   between area (μm^2) and both SBW (μg) and MBW_{area} (μg). Here c.i. stands
520   for "confidence interval". Significant r values (0<c.i.<1) are set in bold.

	Area (μm^2)					
	G. bulloides		*N. incompta*		*G. truncatulinoides*	
	r	c.i.	r	c.i.	r	c.i.
SBW (μg)	**0.72**	0.52, 0.85	**0.57**	0.28, 0.77	**0.62**	0.41, 0.76
MBW_{area} (μg)	0.014	-0.32, 0.35	-0.15	-0.47, 0.21	0.21	-0.09, 0.44

521
522   Furthermore, a Pearson correlation test (see section 3.6) has been carried out in
523   order to assess the influence of area on SBW and MBW_{area} (Table 3). Results
524   showed that the SBWs from the three species correlated positively and significantly
525   (0< c.i <1). With their corresponding areas (0.57< r <0.72). Concerning the MBWs,
526   no significant (0> c.i. >1) correlations with the area are observed (-0.15< r <0.2).
527   Therefore, these correlations further highlight the fact that SBW values are
528   significantly influenced by shell area, while MBW_{area} values appeared to be
529   independent of the area.
530   Differences between SBW and both MBW_{area} vary depending on the species: SBW
531   is slightly heavier for *G. bulloides*, heavier for *N. incompta* and lighter for *G.*
532   *truncatulinoides*. The mean standard deviation for all 3 species is around 8%: 7.8%
533   for *G. bulloides*, 6.4% for *N. incompta* and 13% for *G. truncatulinoides*. We take
534   these values as the error adjustment for SBW in the different size fractions (250-300
535   μm, 200-250 μm and 400-500 μm respectively). It is difficult to compare these results
536   with other studies as size fractions and species are often different, but this error
537   estimates are in the same order of magnitude as some other MBW published in core-
538   tops records and sediment traps (de Moel et al., 2009; Moy et al., 2009).
539   These findings highlight the fact that the use of sieve fractions does not provide
540   enough control on the influence of morphometric parameters in test weight.
541   Morphometric variations described in Table 1 indicate that the typically used sieve
542   fractions may be unreliable due to the number of individuals out of the desired
543   fractions and the variability within the size range. The correlations between SBW
544   and shell area are consistent with previous studies (Aldridge et al., 2012; Beer et al.,
545   2010) and underscore the importance of isolating the component of variation in

546 foraminifera shell thickness that represents a change in calcification and does not
547 occur as a direct result of change in shell size. Thus, the shell weight was size-
548 normalized after Beer et al., (2010) by isolating the influence of isometric scaling on
549 wall thickness and calcification density.
550 Moreover, both MBW_{area} (Fig. 2) and MBW_{diam}, in either the sediment trap data and
551 core-top data, do not correlate with area and diameter ($1x10^{-5} < r^2 < 0.33$ and 0.001
552 $< r^2 < 0.2$ respectively) indicating that size does not have an influence on these
553 values. This suggests that our size-normalization procedure adequately removes the
554 size influence (Fig. 2) and therefore, our MBW data represents a robust parameter
555 reflecting test wall thickness and calcification intensity not influenced by test size
556 (Table 3). Therefore, MBWs can be considered as a reliable calcification intensity
557 proxy.
558 Based on all the above, from this point we'll focus our discussion on the MBW_{area} to
559 discuss the foraminifera shell weight variability on seasonal, interannual and pre to
560 post-industrial Holocene time scales.
561
562 **4.2. Seasonal variations of foraminifera calcification in the NW Mediterranean**
563 MBW_{area} values were calculated for the three species to illustrate the seasonal
564 variability of these parameters (Figs. 3 and 4). Samples have been assigned to their
565 corresponding month according to the mean cup sampling date.

566
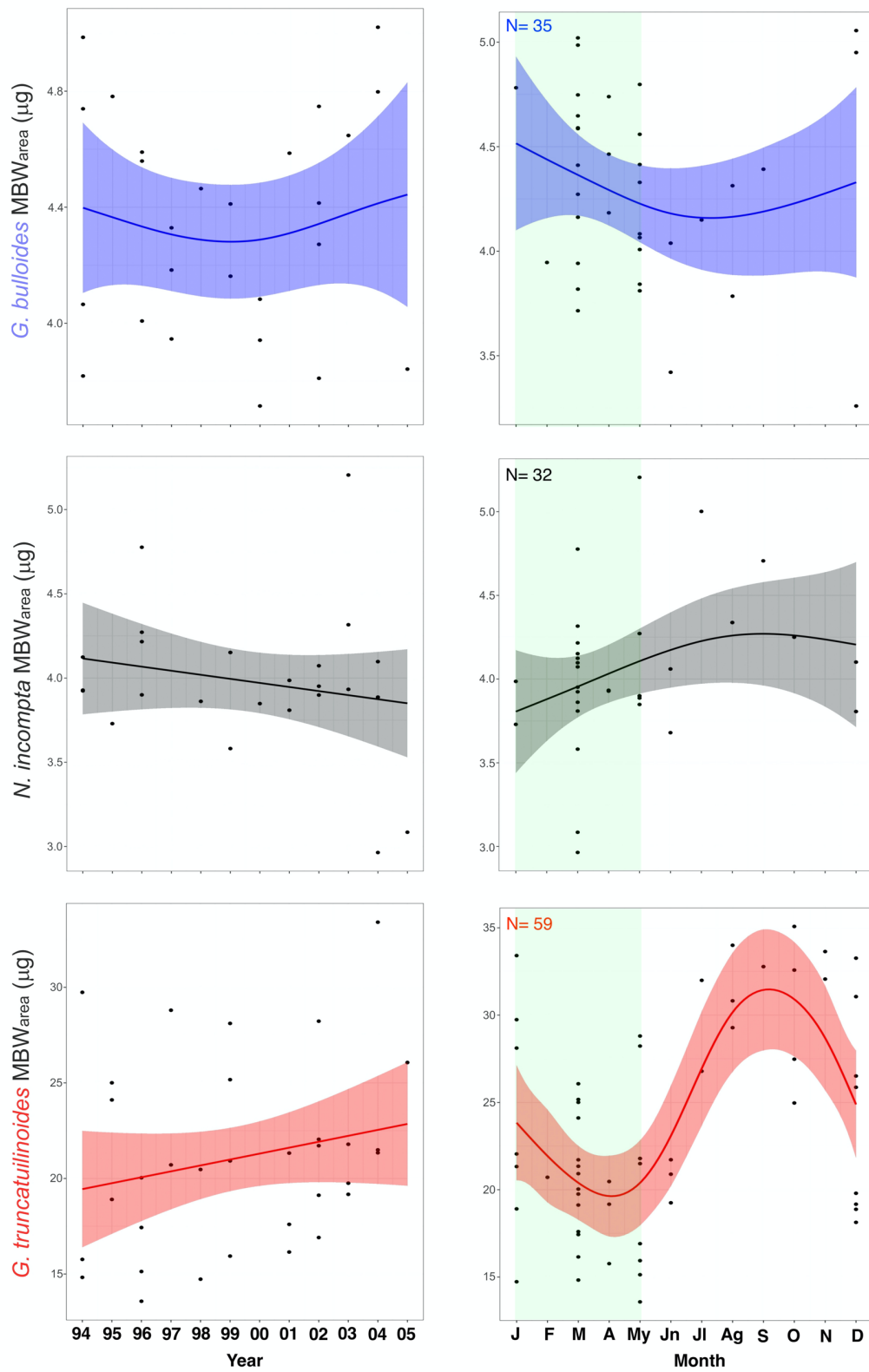
Figure 3. Mean MBW$_{area}$ (µg) values across the years and for a composite year for *G. bulloides, N. incompta* and *G. truncatulinoides* in the Planier

569   sediment trap. Light-green shaded area represents the high productivity
570   period in the study zone (Rigual-Hernández et al., 2012).

571 The mean MBW_{area} for the three species in the Planier sediment trap are 4.29 μg ($\pm$
572 0.45 μg for *G. bulloides*, 4.04 μg ($\pm$ 0.4 μg) for *N. incompta* and 23.25 μg ($\pm$ 6.2 μg)
573 for *G. truncatulinoides*. The seasonal variations in shell calcification differ according
574 to the species.

575 In the case of *G. bulloides*, maximum annual calcification values are reached during
576 winter and early spring: 5.05 in December and 5.02 μg in March. January displays
577 the highest mean value: 4.78 μg. Minimum values are reached during summer: 3.72
578 μg in June, which is also the month that exhibits the lowest mean MBW_{area}. Overall,
579 there is a 1 μg seasonal difference in calcification between maximum and minimum
580 values, which corresponds to a 24.5% change in the mean MBW_{area} value. Mean
581 seasonal standard deviation is $\pm$ 0.47 μg.

582 *N. incompta* shows a maximum in calcification in late spring to mid-summer: a
583 maximum value of 5 μg is reached in May, while July is the month that displays the
584 highest mean value (5 μg). Lowest values are reached in early spring: 2.96 μg in
585 March, while January displays the lowest mean value (3.85 μg). Thus, the annual
586 mean seasonal amplitude is 1.15 μg which translates into a 28% seasonal MBW_{area}
587 variability. Standard deviation is $\pm$ 0.28 μg.

588 Finally, *G. truncatulinoides* displays a seasonal maximum MBW_{area} value in late
589 summer-autumn, with a maximum reached in October: 35.07 μg, while November;
590 is the month that shows the highest mean MBW_{area} value (32.85 μg). The lowest
591 value is reached in March: 13.57 μg, and April is the month that shows the lowest
592 mean value: 18.45 μg. Seasonal MBW_{area} difference is 14.3 μg: a 60% variability.
593 Mean typical seasonal deviation is $\pm$ 3.7 μg.

594

595 **4.3. Interannual MBW_{area} trends**

596 Trends throughout the 12-year record are represented in Figs. 3 and 5. In order to
597 obtain representative data for each year, maximize data availability of each species
598 and avoid the impact of months with insufficient specimens on the interannual trends,
599 only MBWs from the productive period (January to May) of each year analyzed were
600 included.

601 *G. bulloides* MBW_{area} showed a slight decrease from 1994 to 2000 and a slight
602 increase from 2000 to 2006. Over the studied interval, the lowest value is reached
603 in the year 2000 and the highest in 2004. Lowest mean annual values were reached
604 during years 2000 and 2005 (3.9 and 3.85 μg, respectively).

605 On the other hand, *N. incompta* MBW_{area} showed a slight calcification reduction with
606 the highest variability in recent years. Both maximum and minimum values are

607 displayed in recent years: 2004 and 2005 respectively. Mean yearly MBW$_{area}$ values
608 reach a maximum in 2003 (4.4 µg) and a minimum in 2005 (3.2 µg).
609 Finally, *G. truncatulinoides* MBW$_{area}$ displayed a different pattern, with an overall
610 steep calcification increase throughout the record. Minimum calcification values are
611 observed in 1996, which is also the year with the lowest mean MBW$_{area}$ (16.5 µg)
612 observed. Maximum value is displayed in 2003, and its mean value is also the
613 highest of the record (26.1 µg).
614 All environmental parameters showed variations across the years. Sea Surface
615 Temperatures (SSTs) displayed a slight but constant decrease over the years, while
616 salinity showed a slight increase, mainly since 2002. From late 2000 until late 2002,
617 phosphate and nitrate concentrations were exceptionally low (Fig. 5). This feature
618 has already been described in the Gulf of Lions (Meier et al., 2014). Between the 2
619 periods for which direct *in situ* carbonate system parameters measurements were
620 available, 1998 to 2000 and 2003 to 2005 (Fig. 5), CO_3^{2-} dropped by 10-15 µmol/kg,
621 DIC increased by 40 to 60 µmol/kg, leading to a pH decrease of 0.02 to 0.025.
622
623 **4.4. Sediment trap, core tops and sediment cores MBW patterns**
624 Foraminifera weights analyzed in core tops and sediment cores from the NW part of
625 the Mediterranean (Fig. 6) and radiocarbon dating allowed a further insight on
626 foraminifera calcification during the Holocene.
627 Flux-weighted MBWs (see section 3.4) from Planier sediment trap for the three
628 planktic species were 4.1 µg for *G. bulloides*, 3.3 µg for *N. incompta* and 22.3 µg for
629 *G. truncatulinoides* (Fig. 6).
630 Data from Planier core-top showed higher mean MBW$_{area}$ values: 5.3 µg, 4.65 µg
631 and 35.4 µg. ^{14}C dating carried out in this core-top was out of the calibration range
632 (see section 3.7 for more details), implying that this sample could be considered
633 post-industrial. Compared to the flux-weighted MBWs from the sediment trap, *G.*
634 *bulloides* weight has been reduced by 1.2 µg, *N. incompta* by 1.3 µg and *G.*
635 *truncatulinoides* by 12-13 µg.
636 Located west of Planier site, Lacaze Duthiers sediment core mean MBWs were:
637 4.99 µg for *G. bulloides*, 4.14 µg for *N. incompta*, and 32.9 µg for *G. truncatulinoides.*
638 ^{14}C analysis displayed a post-industrial age (see section 3.7) for this sample and
639 corresponding MBWs from this sample for *G. bulloides*, *N. incompta* and *G.*
640 *truncatulinoides* respectively were: 4.7 µg, 4.2 µg and 34 µg. Overall, compared to
641 the data from the sediment trap, this corresponds to a 0.6 µg weight loss for *G.*
642 *bulloides*, 0.9 µg for *N. incompta* and 12.2 µg for *G. truncatulinoides* in.
643 Finally, in the Gulf of Minorca, northwest of Planier site, Minorca sediment core mean
644 MBWs were: 5.4 µg for *G. bulloides*, 4.5 µg for *N. incompta* and 36.3 µg for *G.*

645 *truncatulinoides* (Fig. 6). [14]C dating on this core top was carried out on an
646 intermediate depth (see section 3.7) due to the lack of availability of enough
647 specimens in the core-top and displayed a date of 1560 calendar years BP (Table
648 1). Corresponding MBWs for this sample were 5.4 μg, 4.9 μg, 38.2 μg for the three
649 species. Therefore, the weight reduction compared to the sediment trap flux-
650 weighted MBWs are: 1.3 μg for *G. bulloides*, 1.6 μg for *N. incompta* and finally, 16 μg
651 for *G. truncatulinoides.*

652 **Table 4.** Mann-Whitney variance test results between the MBW_{area} of the
653 different sites for the three species. Significant values (p<0.05) are set in bold.

		PLA ST	PLA CT	LCD SC	MR 3.1.A
				MBW_{area}	
G. bulloides					
PLA ST			0.110	**0.003**	**7.86e^{-13}**
PLA CT	MBW_{area}	0.110		1	1
LCD SC		**0.003**	1		0.114
MIN SC		**7.86e^{-14}**	1	0.114	
N. incompta					
PLA ST			0.438	0.890	**2.59e^{-5}**
PLA CT	MBW_{area}	0.438		0.342	1
LCD SC		0.890	0.342		**0.034**
MIN SC		**2.59e^{-5}**	1	**0.03**	
G. truncatulinoides					
PLA ST			0.120	**0.003**	**3.13e^{-15}**
PLA CT	MBW_{area}	0.120		0.644	1
LCD SC		**0.003**	0.644		**0.01316**
MIN SC		**3.13e^{-15}**	1	**0.013**	

654

655 A Mann-Whitney variance test (see section 3.6) was carried out in order to analyze
656 the variance between the different MBW_{area} datasets (Table 4) from the different
657 sites. MBW_{area} data from the sediment trap appeared to have a significantly different
658 variance compared to the MBW_{area} from Menorca sediment core for the three
659 species ($3.13e^{-15} < p < 2.59e^{-5}$), however, differences between the sediment trap data
660 and the with Lacaze-Duthiers sediment core were only significant for *G. bulloides*
661 and *G. truncatulinoides* (p=0.003). Concerning differences between the Planier
662 sediment trap and the underlying core-top, no significant differences were observed
663 for any of the species (0.11<p<0.438), most likely due to the small number of

664 samples from the latter site: only 2 samples were available. Note that the differences
665 between the sediment cores MBW$_{area}$ datasets differed according to the site and
666 species. In the case of *G. bulloides*, no significant differences were observed
667 between Planier core-top, Lacaze-Duthiers sediment core and Menorca sediment
668 core. In the case of *N. incompta* and *G. truncatulinoides*, differences between
669 Lacaze-Duthiers and Menorca sediment core are significant (0.013<p<0.03),
670 although on lower orders of magnitude compared to the differences between the
671 sediment trap and sediment cores datasets (Table 4). This demonstrates that the
672 difference between the sediment trap MBW$_{area}$ dataset and the seabed sediments
673 MBW$_{area}$ datasets was greater than the difference between the different seabed
674 MBW$_{area}$ datasets.

675 ## 5. Discussion
676

677 **5.1. Seasonal controls on planktic foraminifera shell calcification in the NW**
678 **Mediterranean**
679 As described in section 4.2, the seasonal variability of MBW$_{area}$ displays important
680 differences across the three species analyzed. The different seasonal pattern in
681 MBW$_{area}$ is reflected by the lack of correlation between the seasonal patterns of
682 MBW$_{area}$ of the different species, i.e., r= -0.23 (p>0.05) between *G. bulloides* and *N.*
683 *incompta* and r= 0.16 (p>0.05) between *G. bulloides* and *G. truncatulinoides*. Only
684 the seasonality of *N. incompta* MBW$_{area}$ and *G. truncatulinoides* MBW$_{area}$ share some
685 similarities, as reflected in the significant and positive correlation (r= 0.66; p<0.05).
686 In order to examine the main controls on foraminifera seasonal calcification in the
687 Gulf of Lions, here we compare the seasonal variability of planktic foraminifera
688 calcification with foraminifera fluxes previously estimated for the Planier sediment
689 trap (Rigual-Hernández et al., 2012) satellite data for the studied site and a suite of
690 environmental parameters measured at the DYFAMED site (see section 3.4).
691 Furthermore, GAM have been generated for all three species (see Supplementary
692 figs. 3,4 and 5) and the environmental parameters considered here in order to give
693 a further insight on the potential factors controlling the MBW$_{area}$. These models
694 showed that *G. bulloides* and *G. truncatulinoides* seasonal calcification trends are
695 significant (p= 0.05 and p= 2.4e^{-5} respectively). On the other hand, *N. incompta*
696 seasonal trend does not appear to be significant (p= 0.14).

697   **Table 5**. Correlation matrix of seasonal (monthly) test weights and the
698   environmental parameters from Planier (sediment trap and satellite data) and
699   DYFAMED site (see section 3.4). Significant correlations (p<0.05) are set in
700   bold.

Parameters		G. bull.	N. inc.	G. truncat.	G. bull.	N. inc.	G. truncat.	Chl-a	SST	Salinity	[NO₃]	[PO₄]	pH	[CO₃]	[CO₂]
		Planier site data								**DYFAMED site data**					
				MBW$_{area}$		Fluxes									
G. bull.		1	0.232	0.167	0.012	0.027	0.152	0.318	-0.32	-0.163	0.292	0.33	0.096	0.189	0.243
N. inc.	MBW$_{area}$	-0.232	1	**0.667**	**-0.582**	-0.407	-0.405	-0.484	**0.688**	0.368	0.272	0.235	-0.35	0.474	-0.28
G. truncat.		0.167	**0.667**	1	**-0.905**	**-0.725**	**-0.666**	**-0.585**	**0.672**	-0.299	0.258	0.512	0.113	**0.732**	0.541

702

Here, we first approach seasonal shell calcification by considering the Optimum Growth Conditions (OGC). Previous studied have defined these conditions on a wide variety of ways: abundance of foraminifera, the chlorophyll-a concentration and even nutrients concentration (de Villiers, 2004; Schiebel et al., 2001; Schiebel and Hemleben, 2017). Therefore, we aim to explore the impact of these parameters as OGC on the shell calcification.

Among all the environmental parameters, de Villiers; (2004) suggested that shell calcification, and therefore MBWs, is primarily controlled by the OGC that can be defined as the most suitable environmental conditions for the development of a given planktic foraminifera species. Based on the latter study, it could be expected that favorable environmental conditions for foraminifera growth would lead to both greater shell fluxes and enhanced shell calcification. Our correlation analysis shows that only *G. truncatulinoides* displays a significant (and negative) correlation with it's flux (r= -0.66, p>0.05). GAM results (see Supplementary figs. 3, 4 and 5) support these observations, with shell flux showing a stronger effect on the calcification for *G. truncatulinoides* compared to the other two species fluxes.

According to the OGC theory, species calcification patterns vary according to the species and their fluxes. Interestingly, *G. truncatulinoides* calcification correlates negatively and significantly with all three species fluxes, a pattern opposite to what the OGC theory predicts (de Villiers, 2004), i.e., optimum ecological niche is associated with enhanced calcification. Thus, a possible explanation reconciling our observations with the OGC theory may be that *G. truncatulinoides* tends to prioritize energy allocation toward growth and reproduction at the price of a reduced calcification. It is thought to reproduce once a year in winter in subtropical waters and it has been speculated that nutrient availability and the lack of predation could explain this strategy. During this interval, the other major species display low abundances in the water column, which could allow *G. truncatulinoides* to reproduce due to the lack of competition. *N. incompta* calcification displays a similar pattern, a negative correlation with all three species, but with a lower level of significance. It's MBW$_{area}$ correlates negatively and significantly (p<0.05) with *G. bulloides* flux, but

733   its fluxes correlate positively and significantly with the latter species fluxes (see
734   Supplementary table 2). This is interesting, as it may highlight interspecific relations.
735   First, this could lead to the assumption that when *G. bulloides* dominates the
736   assemblages, *N. incompta* also displays a high abundance (Rigual-Hernández et
737   al., 2012). Then, it could show that when conditions are favorable, *N. incompta*
738   reproduces at a higher rate at the price of thinner shells (Table 1). This agrees with
739   *N. incompta* life cycle, which is known to be outnumbered by opportunistic species
740   when nutrients supply is high (Schiebel et al., 2002), but dominate the assemblages
741   when stratified waters are set, therefore, when conditions are favorable or when in
742   cohabitation with opportunistic species, it could focus on its reproduction. Note that
743   *G. truncatulinoides* and *N. incompta* MBW_{area} correlate positively and significantly
744   ($p < 0.05$), showing a similar calcification pattern on a seasonal scale.
745   An alternative proxy for OGC that may be considered is chlorophyll-a concentration.
746   Chlorophyll is considered an indicator of the algal biomass concentration, which is
747   known to represent a large part of some foraminifera species diet (Schiebel and
748   Hemleben, 2017). However, our data only showed a significant correlation of
749   chlorophyll-a with *G. truncatulinoides* calcification. A stronger trend would be
750   expected under the OGC theory for *G. bulloides* as algae are a vital part of its diet
751   (Hemleben et al., 1989; Schiebel and Hemleben, 2017). This lack of correlation
752   between *G. bulloides* and chlorophyll-a has already been described (Weinkauf et al.,
753   2016). We speculate that *G. bulloides* may preferentially feed on certain groups of
754   phytoplankton which changes in seasonal abundance in the photic zone do not
755   necessarily follow the seasonal pattern of total chlorophyll concentration (Marty et
756   al., 2002). Also, note that the chlorophyll-a data presented here only represents the
757   conditions in the surface layer. GAM results further support these observations (see
758   Supplementary fig. 5), with chlorophyll-a showing a significant impact on *G.*
759   *truncatulinoides* calcification. This observation indicates that optimum calcification
760   conditions for *G. truncatulinoides* are reached at times of minimum annual algal
761   biomass concentration in the photic zone. It is possible that, due to its deeper habitat
762   (Schiebel and Hemleben, 2017), *G. truncatulinoides* feeds on phytoplankton
763   dwelling in subsurface levels of the water column. In fact, a deep chlorophyll
764   maximum is known to develop during large part of the year in the Northwestern
765   Mediterranean (Estrada et al., 1993) but its presence is not detected by satellites.
766   This interpretation is in agreement with earlier work by Pujol and Vergnaud Grazzini,
767   (1995) who found peak abundances of this species during the summer below the
768   thermocline.

769
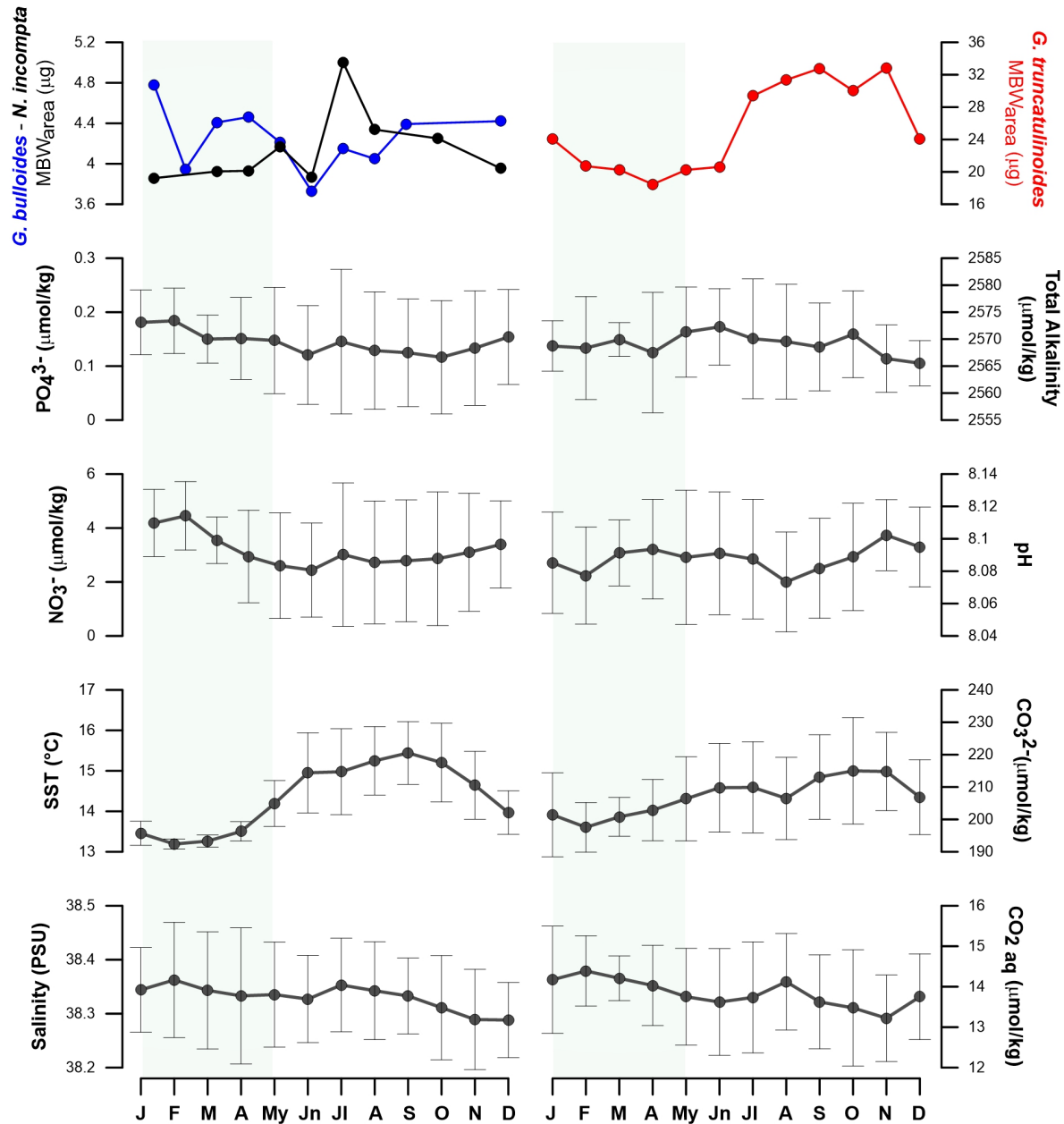
Figure 4. *G. bulloides*, *N. incompta* and *G. truncatulinoides* seasonal mean monthly MBW_area variations compared with Planier environmental data and the resampled seasonal signal of environmental parameters from the DYFAMED site across a composite year.

Previous studies have described that, in those settings where foraminifera abundance covaries with nutrient concentrations, then nutrients are probably a better OGC proxy than chlorophyll concentrations (Schiebel et al., 2001). In turn, the correlation of nutrients (nitrates and phosphates) with fluxes were positive for all three species, although only significant (p<0.05) for *G. truncatulinoides* abundance (r= 0.58 and 0.59 for nitrates and phosphates respectively). Although here we have

780 first described the OGC as species fluxes and then as the chlorophyll-*a*
781 concentration, it is important to remember that the niche and favorable conditions
782 meant to be described by the OGC for each species are multi-dimensional.
783 Note that nitrate and phosphate concentration variations were closely linked to each
784 other (r= 0.876, p<0.05), making it difficult to determine if the resulting effect on
785 foraminifera calcification is due to the effect of a single driver or to the combination
786 of both. Our work shows that nutrient concentrations (both nitrates and phosphates)
787 do not correlate significantly with any of the three species MBW studied, and this
788 observation is supported by the GAM results which do not show any significant effect
789 of nutrients concentrations on the calcification.
790 Previous studies have suggested that salinity may have an influence on foraminifera
791 calcification (Zarkogiannis et al., 2022). However, our data suggest that the role of
792 salinity on calcification in our study region is unlikely since its seasonal amplitude is
793 tiny (0.1 PSU; Fig. 4). This idea is supported by the lack of correlation between
794 salinity and MBW$_{area}$ for the three species studied (Table 5) and the GAM results.
795 Temperature (Sea Surface Temperature) has been described as a major factor that
796 controls the size (Schmidt et al., 2004) and porosity (Burke et al., 2018) of planktic
797 foraminifera, therefore it could represent a major control factor on shell calcification
798 in the NW Mediterranean. In particular, calcification could be positively linked to
799 temperature through different mechanisms: (i) warmer temperatures have been
800 shown to increase enzymatic activity and therefore enhanced growth and
801 calcification rates (Spero et al., 1991); (ii) Lombard et al., (2011) stated that higher
802 temperatures could also increase feeding and ingestion rates, but it remains unclear
803 if this could result in a calcification rate increase. Our data revealed that SST
804 correlates positively and significantly with *N. incompta* and *G. truncatulinoides*
805 calcification (r= 0.69 and 0.67 respectively, p<0.05). GAM results also displayed a
806 positive and the most significative effect of the SST on these two species. These
807 findings highlight that SSTs are one of the main factors affecting *N. incompta* and *G.*
808 *truncatulinoides* calcification among the parameters considered here. Finally, in
809 addition to having an impact on the size and calcification of the planktic foraminifera,
810 temperature is well known as a major control of the carbonate system, due to the
811 increased solubility of atmospheric CO_2 at lower temperatures, and therefore it could
812 have an indirect effect on foraminifera calcification by affecting the carbonate
813 system.
814 Data for the carbonate system were only available for years 1998 to 2000 and 2003
815 to 2005 and, therefore gaps comprised in these years were filled with estimates
816 using the CO2sys macro (see section 3.6 for more details). However, note that the
817 data available for these parameters was relatively smaller compared to the other
818 parameters and may have prevented detection of other significant relationships. The

819   relationship between CO_3^{2-} and MBW has been described in previous studies
820   (Barker and Elderfield, 2002; Marshall et al., 2013) and the bulk of evidence indicates
821   that foraminifera MBWs to be positively linked with CO_3^{2-} concentrations (Aldridge et
822   al., 2012; Osborne et al., 2016). However, it appeared that planktic foraminifera
823   response to CO_3^{2-} concentration was not uniform and varied across species (Beer
824   et al., 2010; Lombard et al., 2010). The trends between carbonate system
825   parameters and MBWs were similar to those observed when comparing MBWs with
826   temperature, highlighting the covariations between these two parameters (Fig. 4).
827   Our data showed that CO_3^{2-} concentrations were only significantly correlated with *G.*
828   *truncatulinoides* MBW_{area} (r= 0.73, p<0.05), implying that carbonate availability may
829   represent a key control on this species in the Northwestern Mediterranean. On the
830   other hand, GAM result (see Supplementary figs. 3, 4 and 5) did not show a
831   significant impact of any carbonate system parameters for any of the three species
832   calcification. As stated previously, the lack of data could have prevented the
833   detection of further trends, but considering the seasonal patterns of carbonate
834   system parameters, a potential role of the CO_3^{2-} concentration could be expected.
835   In summary, seasonal correlations, trends and GAM showed that the environmental
836   parameters that displayed the highest correlation with MBW_{area} vary according to the
837   species. *G. bulloides* calcification appeared to be affected mainly by the OGC and
838   interspecific relations. *N. incompta* calcification showed to be mainly positively linked
839   to the SST. Finally, *G. truncatulinoides* calcification was positively linked with the
840   SST and potentially CO_3^{2-} concentration, while OGC displayed a negative effect on
841   its MBW_{area}. The combined effect of these parameters seems to control foraminifera
842   calcification in the Gulf of Lions; however, it should be considered that covariation
843   between these parameters is strong, and therefore it is difficult to isolate the effect
844   of a single parameter. Moreover, it is likely that the ecology and life cycle of the
845   species could also be a major factor affecting the response of the species
846   calcification to the environmental parameters variations. Our results are in
847   agreement with earlier studies that stated that OGC (de Villiers, 2004), SST and
848   CO_3^{2-} (de Villiers, 2004; Marshall et al., 2013; Osborne et al., 2016) concentrations
849   are the main factors that impact calcification in planktic foraminifera, while the
850   calcification response to those parameters is species-specific, which is in agreement
851   with the work of Weinkauf et al, (2016).
852

853   **5.2. Interannual trends in planktic foraminifera calcification**
854   As stated previously, the Mediterranean Sea is a sensitive zone to atmospheric CO_2
855   accumulation (Ziveri, 2012) and is experiencing ongoing ocean acidification. On an
856   interannual time scale, different studies (Beer et al., 2010; Osborne et al., 2016)
857   have shown that sea surface warming and carbonate system parameters are the

858 most likely parameters to control calcification on key calcifying phytoplankton
859 species such as the coccolithophore *Emiliania huxleyi* organisms (Meier et al.,
860 2014). However, datasets from sediment traps that cover a wide span of years and
861 in which foraminifera weights have been analyzed are rare (Kiss et al., 2021),
862 therefore it is difficult to place our results in a more global context. Our GAM results
863 (see Supplementary figs. 3 and 4) showed that both *G. bulloides* and *N. incompta*
864 interannual patterns were non-significant. This is not surprising as the calcification
865 trends for these two species did not display a clear and marked variation over the
866 years, excepting a small mean calcification reduction (Fig. 3) and minimum
867 calcification values in 2004 and 2005 (Fig. 3 and Supplementary figs. 3 and 4).

868
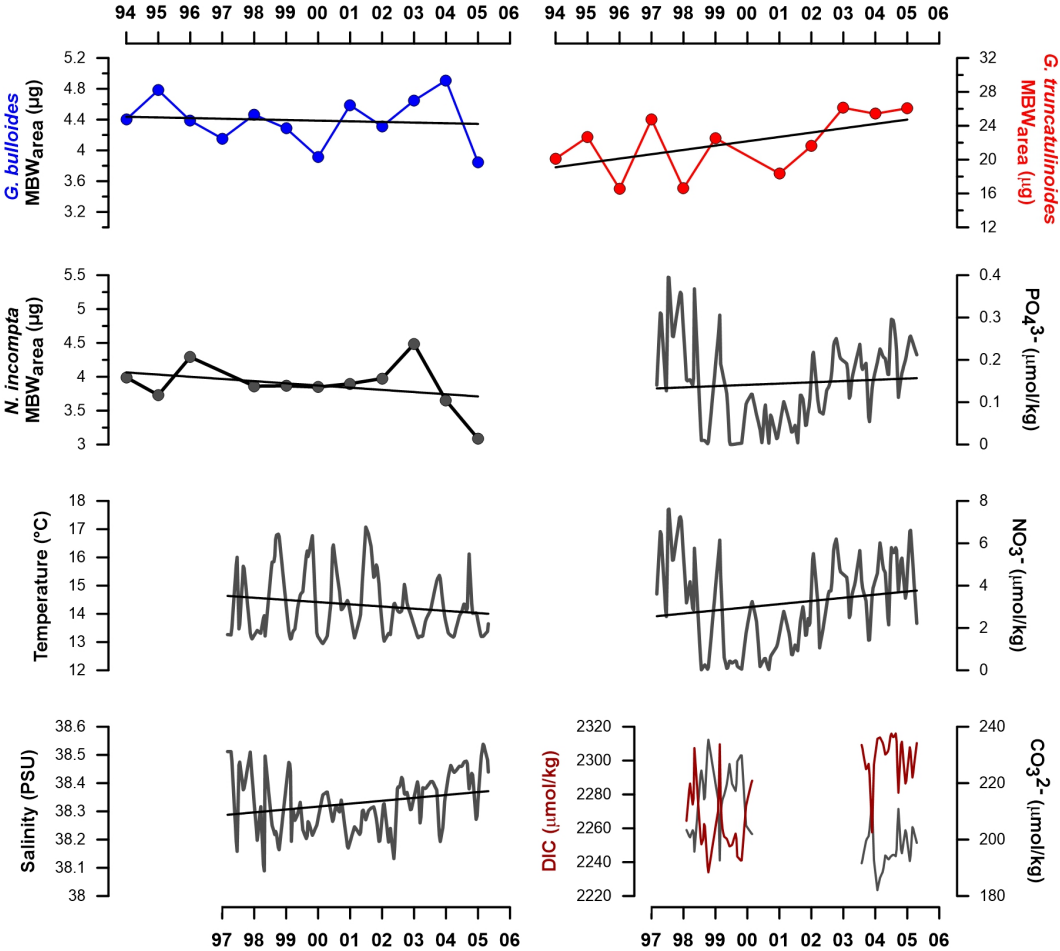
869 **Figure 5.** Interannual mean MBW$_{area}$ (μg) values for *G. bulloides*, *N. incompta*
870 and *G. truncatulinoides* from the high productivity period (see section 2) and
871 Planier and DYFAMED environmental data variations across the record.
872 Black lines represent the trends from the MBW$_{area}$ and resampled data. DIC
873 represents "Dissolved Inorganic Carbon".

874 Notably, the trend in *G. truncatulinoides* is opposed to the previous two species and
875 shows a steady and steep increase throughout our record. Over the analyzed time

876 span, its MBW increased around 20% (equivalent to an increase of ~5 μg).
877 According to the GAM results, the interannual calcification trend for this species is
878 significant (see Supplementary fig. 5). If this calcification increase continues on
879 current trends, then the average MBW of *G. truncatulinoides* will double by 2024.
880 Analysis of present *G. truncatulinoides* populations is urgently needed to assess if
881 the observed trend held true during the last two decades. It is important to note that
882 while *G. truncatulinoides* seems to exhibit a positive correlation with CO_3^{2-}
883 concentration on a seasonal scale, no clear correlation was found with the
884 interannual changes of CO_3^{2-} concentration. This feature is also supported by the
885 GAM results. A similar enhancement in shell calcification has been described in the
886 Balearic Sea for *G. truncatulinoides* in high-resolution sediment cores (Pallacks et
887 al., 2020), but also in *Globorotalia inflata*. Taken together, our observations and the
888 study mentioned above, suggest that deep dwellers are unaffected by the recent
889 ocean acidification and changes in the carbonate system and that the recent change
890 in one or several environmental drivers may be stimulating the calcification of these
891 species.
892 Here, we theorize that the interannual patterns presented in Figs. 3 and 5 mainly
893 reflect the seasonal changes in the regional oceanographic setting. As described
894 previously (see section 2 for more details), the Gulf of Lions is influenced by a strong
895 seasonality. The recent SST decrease could be linked to an enhancement in water
896 mixing, as cold and deep salty water reach up to the surface. This mechanism would
897 be less intense during years 2000 to 2002, corresponding to a SST increase along
898 with a salinity decrease and absolute minimums in nutrients concentrations (Fig. 5),
899 as water stratificates, these are consumed by primary production. Finally, in recent
900 years, water mixing seems to be reactivated, as SST keeps decreasing and nutrients
901 concentrations increase again. This mechanism also affects the carbonate system
902 parameters, as water mixing brings to surface deeper DIC enriched waters to the
903 surface, coupled with a $[CO_3^{2-}]$ reduction. Our data shows that alkalinity patterns
904 display similar tendencies to DIC, however, until the second time span covered by
905 carbonate system data, alkalinity variations are proportionally higher than DIC
906 variations (see Supplementary material), suggesting a water mixing phenomenon.
907 On the other hand, DIC variations turn to be higher than alkalinity variations from
908 2003 to 2005, suggesting an additional effect of carbon inputs on the carbonate
909 system not reflected in the alkalinity data.
910 Note that SSTs, despite showing a positive and significant correlation with *N.*
911 *incompta* and *G. truncatulinoides* on a seasonal scale and the GAM showing a
912 positive and significant effect on the calcification, did not follow the same pattern as
913 the latter species. This observation implies that other mechanisms or parameters
914 than the ones considered here may be affecting the MBW$_{area}$ on recent years.

 5.3. Holocene core-top data comparison

916
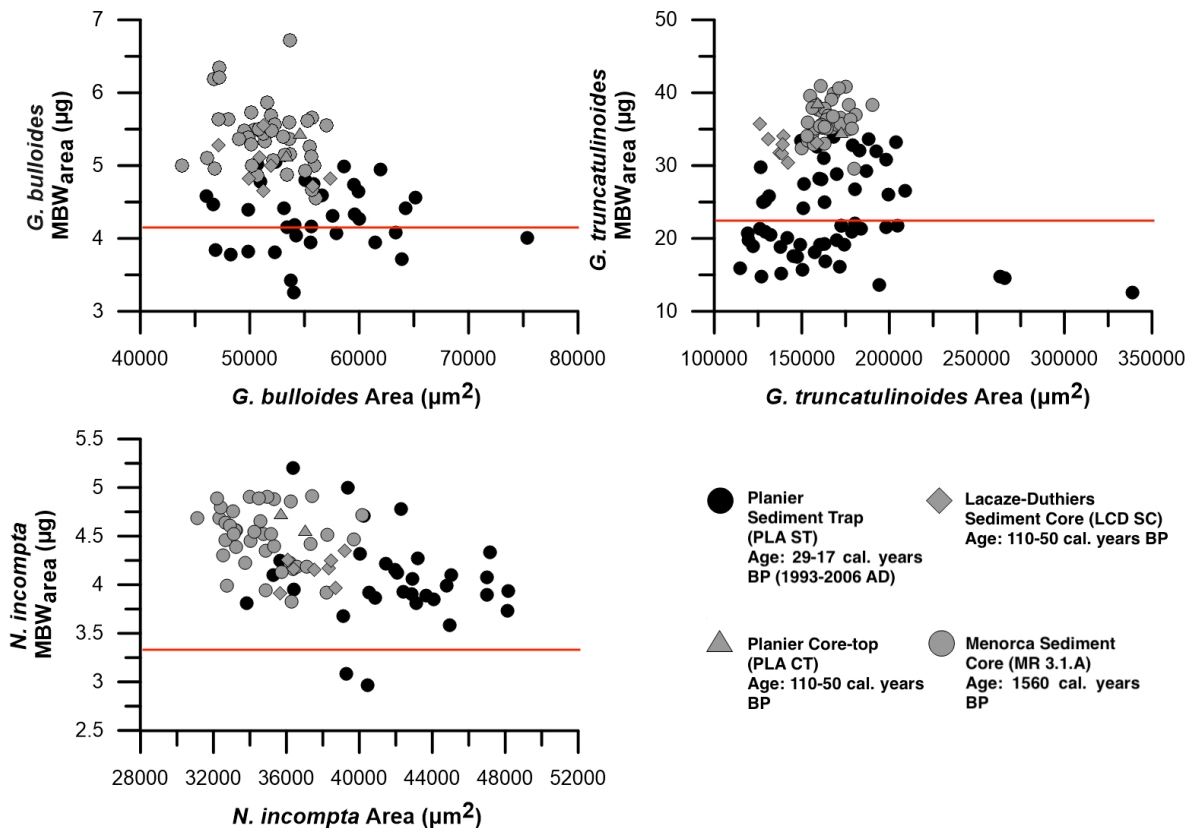
918 **Figure 6.** MBW$_{area}$ in μg and area in μm2 comparison in the sediment trap (PLA ST),
919 Planier core-top (PLA CT), and both Lacaze-Duthiers (LCD SC) and Minorca sediment
920 core (MR 3.1.A). Black dots represent data from the sediment trap, while lighter colors
921 represent data from the different seabed sediments. Red lines represent the flux-
922 weighted values from the sediment trap.

923

924 The comparison of the well-preserved assemblages of planktic foraminifera in the
925 pre-industrial and industrial Holocene-aged surface sediments with those collected
926 by a long-sediment trap record offers a unique opportunity to assess the impact of
927 recent environmental change on the calcification of calcareous zooplankton in the
928 Mediterranean Sea (Fig. 6). However, when comparing data from sediment traps
929 and seabed sediments, the possible role of calcite dissolution must be taken into
930 account.

931 Calcite dissolution in the water column and/or on the sea floor could be invoked as
932 a source of variability between the sediment trap and surface sediment data sets
933 (e.g., Dittert et al., 1999). Therefore, in order to obtain meaningful interpretations
934 from our data sets it is important to assess the possible role of dissolution in the
935 preservation of planktic foraminifera shells. Several lines of evidence suggest,
936 however, that calcite preservation does not represent an important source of bias in

937 our study area. Firstly, the Mediterranean Sea is supersaturated with respect to
938 calcite (Millero et al., 1979) and the location of all the analyzed samples is much
939 shallower than the location of the calcite saturation horizon (Álvarez et al., 2014),
940 therefore, calcite dissolution seems unlikely (Schneider et al., 2007). Secondly,
941 several sediment trap studies have documented that calcareous plankton
942 experience negligible dissolution in their transit from the surface ocean to the sea
943 floor (Beaufort et al., 2007; Moy et al., 2009; Rigual-Hernández et al., 2020). Thirdly,
944 SEM and microscopic observations of all 3 species in samples from both the
945 sediment traps and sediment cores showed no sign of dissolution and foraminifera
946 were well preserved (see Supplementary fig. 6). These arguments suggest that
947 calcite dissolution does not represent an important control in the weight of the
948 planktic foraminifer shells in the analyzed samples. However, it has been
949 documented that when dissolution takes place, the thinnest shells are affected first
950 (Berger, 1970) while the heaviest and more calcified specimens remain. In our study,
951 the specimens from the sediment trap were lighter that the ones from the sediment
952 cores, which corresponds to the previous statement. This is important to
953 acknowledge as the individuals from the seabed sediment could only represent more
954 calcified and solid individuals, while the most fragile and less calcified individuals
955 may not have been preserved. Therefore dissolution cannot be completely ruled out
956 here as a possible source of variability between the surface sediment and sediment
957 trap data sets.
958 Overall, the lower shell weights of the foraminifera collected by the traps suggests
959 that the three planktic foraminifera species may have experienced a reduction in
960 their calcification since pre-industrial times to post-industrial and recent Holocene.
961 While the shell weight of each species measured in the sediments show some
962 variability across seabed sediments (Fig. 6), our data suggest an overall reduction
963 of 18-24% for *G. bulloides*, 20-27% for *N. incompta*, and 32-40% for *G.*
964 *truncatulinoides.* It is important to note that the range of shell weight variability across
965 core-tops and sediment cores (4.5-6.7 μg and 0.37 μg typical deviation for *G.*
966 *bulloides*, 3.8-4.9 μg and 0.23 μg typical deviation for *N.incompta*, and 29.5-40.9 μg
967 and 2.6 μg typical deviation for *G. truncatulinoides*) is substantially lower than the
968 difference with the sediment trap data (3-5 μg and 0.5 μg typical deviation for *G.*
969 *bulloides*, 2.9-5.2 μg and 0.5 μg typical deviation for *N. incompta* and 12-35 μg and
970 6 μg typical deviation for *G. truncatulinoides*), implying that the shell weight of recent
971 foraminifera populations for the three species is lower than anywhere in the NW
972 Mediterranean in the pre-industrial and post-industrial times. The source of the
973 variability across core tops and sediment cores is most likely caused by the different
974 age of the samples, ranging from 1560 cal. years BP at Minorca mid-depth (Table

975 1) sample to post-industrial at Planier and Lacaze-Duthiers core-tops, and the
976 different environments associated to the location of each core top.

977 A non-parametric two-way Mann-Whitney test (see sections 3.6 and 4.3) showed
978 that the sediment trap MBW_{area} dataset was significantly different ($p<0.05$) from MR
979 3.1.A and non-different from PLA CT for all three species studied here (Table 5).

980 Something to consider when comparing recent sediment trap data with pre-industrial
981 Holocene data is the life cycle of the species. As all the species analyzed presented
982 a lighter weight in the sediment traps, the degree to which the different specimens
983 responded varied. The greatest weight reductions were observed for *G.*
984 *truncatulinoides* populations, while *G. bulloides* populations exhibited the lowest
985 weight loss.

986 Previous work stated that those species hosting photosynthetic algal symbionts
987 exhibit a higher tolerance to environmental changes that may affect their calcification
988 (Lombard et al., 2009). This is due to the fact that these symbionts can modify the
989 sea water chemistry that is in a close range to the shell, allowing a calcification
990 enhancement. Of the species studied here, none are known, with the possible
991 exception of *G. bulloides*, to be symbiont bearing species, therefore, they are among
992 the most vulnerable foraminifera species to any sea water chemistry change.

993 It has been described that some morphotypes of *G. bulloides* do host bacterial
994 endobionts in their cytoplasm (Bird et al., 2017). The later work showed that high
995 amounts of *Synechococcus*, a cyanobacteria, were found in morphotype Id
996 specimens of *G. bulloides* from the California coast. Although no such observations
997 have been reported on morphotype Ib, the dominant *G. bulloides* morphotype in the
998 Mediterranean sea (Schiebel and Hemleben, 2017), this could be relevant as
999 bacterial photosynthetic activity would interact on the close range seawater
1000 chemistry by removing $^{12}CO_2$ and therefore impacting the $^{13}C/^{12}C$ ratios in the
1001 surrounding dissolved CO_2. Moy et al., (2009) work in the Southern Ocean, showed
1002 a 30-35% calcification reduction for *G. bulloides* during the industrial era. Our study
1003 shows that such a similar reduction in *G. bulloides* MBW_{area} (i.e., a mean 20% taking
1004 into account the 3 sites studied) has also taken placed in the Mediterranean Sea.

1005 Even though the species studied were different in Fox et al., (2020), and that shell
1006 thickness was analyzed, that work showed a massive shell reduction for *N. dutertrei*
1007 (around 75%) and a smaller reduction for *G. ruber* (around 20%). *N. incompta* weight
1008 reduction in this study is around 25%, despite that life cycles are different between
1009 these species, our results come in the same line.

1010 Data for *G. truncatulinoides* calcification comparison between pre-industrial and
1011 post-industrial Holocene is scarce. One of the few available studies is the one of
1012 Pallacks et al., (2020) in the western Mediterranean sea using pre-industrial data
1013 and recent foraminifera weight data obtained from high resolution core-tops. *G.*

1014 *truncatulinoides* showed a 24% weight reduction, which is a lower reduction than
1015 what is shown in our study (around 35% MBW_{area} decrease), but shows a similar
1016 trend. Taken together, all these observations suggest that a decrease in major
1017 planktic foraminifera calcification is not only a regional feature but a global scale
1018 process.
1019 On a more regional scale, Hassoun et al., (2015) documented the ongoing changes
1020 in seawater carbonate speciation in the Mediterranean waters. In the latter work, the
1021 distributions of anthropogenic CO_2 showed that all Mediterranean water masses
1022 have already experienced ocean acidification. This effect was more pronounced in
1023 the intermediate to deep masses (300-500m and >500m respectively) in the western
1024 basin, which translated into a minimum pH reduction of 0.1 in this part of the
1025 Mediterranean. As stated previously, over the years in which carbonate parameters
1026 were retrieved from the DYFAMED database, pH was reduced, DIC showed a
1027 marked increase and $[CO_3^{2-}]$ displayed a decrease. Taken together these
1028 observations and our data, it is possible that the observed changes in foraminifera
1029 calcification could have been partially driven by the ongoing ocean acidification in
1030 the Mediterranean.
1031 Moreover, the largest calcification reduction is observed between the seabed
1032 sediments and the sediment trap, this means that the highest calcification reduction
1033 has taken place between post-industrial Holocene and recent Holocene (i.e. the
1034 reduction between LCD SC/PLA CT and PLA ST) (Fig. 6). This could be explained
1035 with the "Great Acceleration theory". The Great Acceleration is a term used to
1036 describe the trends in CO_2 emissions and the associated temperature changes as
1037 consequences of the human impacts on the atmosphere since the 1950s (Head et
1038 al., 2022a, 2022b).
1039 However, other important changes in physical and chemical parameters co-occur
1040 with ocean acidification, and therefore should be also considered. Based on the
1041 seasonal and interannual patterns of the SST in the Gulf of Lions (Figs. 4 and 5),
1042 temperature trends could also be invoked as a likely parameter to affect calcification
1043 here. As shown by the correlations (Table 5) and the GAM results, SSTs are one of
1044 the most likely parameters to affect calcification on different timescales. However,
1045 on a pre-industrial to post-industrial timescale, the effect of the SST on the
1046 foraminifera calcification on longer time scales may be hard to evaluate due to the
1047 effect of the latter on the carbonate system parameters such as CO_2 and CO_3^{2-}
1048 concentration in the water. But note that the Mediterranean is considered to be
1049 warming at a faster rate than the global average (Hassoun et al., 2015; Lazzari et
1050 al., 2014).
1051 Calcification data from the sediment trap has been flux-weighted (see section 3.4) in
1052 order to be compared with the sedimentary calcification data, therefore, this data

1053 could be affected by a change in the incoming foraminifera flux (de Moel et al., 2009).
1054 In this line, the Gulf of Lions, presents a marked seasonality (see section 2) and the
1055 both the mass fluxes (Heussner et al., 2006) and foraminifera fluxes present strong
1056 seasonal variations. Parameters such as the North Atlantic Oscillation index, the
1057 river runoff and the intensity of the seasonal water cascading process have been
1058 suggested to play a role on planktic foraminifera production and export (Rigual-
1059 Hernández et al., 2012). The later study shows that most of the species flux showed
1060 a yearly uni-modal distribution, but the flux values and distribution remained fairly
1061 constant over the years. This highlights that, in our study zone, a major change in
1062 the foraminifera flux affecting the flux-weighted calcification value is unlikely.
1063 In summary, our results suggest that the interactive effect of rising ocean acidity,
1064 and enhanced SST (regionally amplified in the NW Mediterranean, (Hassoun et al.,
1065 2022, 2015)) represent the most likely responsible factors for the MBW differences
1066 between the pre-industrial and post-industrial to recent Holocene. However, the
1067 analysis of seasonal and interannual trends indicates that the influence of these
1068 parameters is species-specific and varies across the studied time scales. This
1069 implies that the controls of planktonic foraminifera are complex and that factors other
1070 than ocean acidification and warming are likely to also account for part of the
1071 variability observed between sediment trap and seabed sediments.
1072
1073 **5.4. Influence of environmental variability on MBW$_{area}$ across different time**
1074 **scales**
1075 Our results show that the influence of environmental parameters over the different
1076 time scales studied is not constant and depends on the species, the environmental
1077 driver and timescale.
1078 In the case of *G. bulloides*, our data suggest that OGC and inter-specific
1079 relationships seem to affect its MBW on a seasonal scale, carbonate system seems
1080 to play a major role while on an interannual and on a pre/post-industrial time scales.
1081 *N. incompta* calcification seems affected by OGC, inter-specific relationships and
1082 SST on a seasonal scale, while on longer time-scales carbonate system appears to
1083 play preponderant role. Finally, *G. truncatulinoides* calcification seems positively
1084 correlated to carbonate system and SSTs and negatively with the OGC on a
1085 seasonal scale. However, these patterns seem to have an opposite effect on an
1086 interannual scale, as *G. truncatulinoides* calcification shows a clear increase while
1087 carbonate system parameters become less and less favorable for calcification. In
1088 turn, on a pre/post-industrial Holocene time scale, its MBW$_{area}$ seem to be affected
1089 by regional processes such as OA and warming.
1090 Factors such as changes in the regional oceanographic processes (Cisneros et al.,
1091 2019; Durrieu de Madron et al., 2017) affect the physical and chemical properties of

1092   the water column and hence, could impact the life cycle of the species studied here.
1093   Also, while *G. bulloides* can either present regular or encrusted forms; *N. incompta*
1094   and *G. truncatulinoides* are crust forming species. In our study, *G. bulloides*
1095   individuals are mainly regular forms, but encrusted individuals were identified in both
1096   the sediment trap and seabed sediments. It is out of the scope of this work to focus
1097   on the effect of the crust on the species MBW, however, Osborne et al., (2016) study
1098   showed that encrusted *G. bulloides* individuals are around 20-30% heavier than the
1099   regular ones.

6. Conclusions

1101

1102   The variability in shell calcification of three planktic foraminifera species (*G.*
1103   *bulloides*, *N. incompta* and *G. truncatulinoides*) was studied in the northwestern
1104   Mediterranean Sea at different time scales using sediment trap and seabed samples.
1105   The analysis of 273 samples and more than 4000 individuals revealed that:

i.   The Sieve Based Weight (SBW) method is not a reliable tool as calcification indicator due to the influence of morphometric parameters on foraminifera weight. The Measured Based Weight (MBW) technique, on the other hand, shows little to negligible influence of the morphometric parameters, and therefore, can be considered a reliable calcification proxy.

ii.   Analysis of the seasonal variability of planktic foraminifera calcification revealed important differences between species. *G. bulloides* exhibited peak calcification during winter, *N. incompta* during mid-summer and *G. truncatulinoides* during late summer to autumn.

iii.   Interannual analysis suggest that *G. bulloides* and *N. incompta* did not display any significant pattern between 1994 and 2005, on the other hand, *G. truncatulinoides* displays a constant and steady calcification increase over recent years.

iv.   Sediment trap and seabed sediment data comparisons between pre-industrial, post-industrial and recent Holocene assemblages showed that all three species experienced a calcification reduction. Modern *G. bulloides*, *N. incompta* and *G. truncatulinoides* individuals were 18-24%, 20-27% and 32-40% less calcified respectively.

v.   Finally, correlations with environmental parameters and GAM indicate that Optimum Growth Conditions affect positively *G. bulloides* and negatively *G. truncatulinoides* calcification respectively. Sea Surface Temperatures affect positively both *N. incompta* and *G. truncatulinoides* calcification. Finally, CO_3^{2-} concentration is also a likely parameter to influence

1130   positively planktic foraminifera calcification in the Northwestern
1131   Mediterranean. However, calcification appeared to be species-specific
1132   and vary depending on the time scale studied. This may suggest that other
1133   parameters than the ones studied here may play a role in foraminifera
1134   calcification.

1135 As planktic foraminifera represent roughly about 50% of pelagic calcite production
1136 (Schiebel, 2002) in the world's oceans, and therefore, an important component of
1137 the marine carbon cycle, a reduction in the calcification of their shell could induce
1138 important changes in the future carbon cycle with feed-backs on climate. Our results
1139 call for increasing efforts in monitoring planktic foraminifera calcification the
1140 Mediterranean in order to determine if the trends suggested by our data will be
1141 sustained over time.

1142

1143 The Supplement related to this article is available at DOI: 10.17632/4t9x554dwz.1

1144

1145 *Competing interests.* The authors declare that they have no conflict of interest.

1146 *Author contributions.* ASRH, FJS and TMB designed the study. JPT designed Figures 1 and
1147 2 and contributed to data discussion. XDM provided Planier core-top and Lacaze-Duthiers
1148 seabed sediment samples. IC provided the Minorca promontory seabed sediment samples.
1149 NH carried out the ^{14}C measurements. AH performed the numerical analyses and
1150 contributed to their interpretations. TMB led the sample processing as well as the
1151 microscopy and image analysis, the foraminifera study and wrote the manuscript with
1152 feedback from all authors.

1153 *Acknowledgments.* Authors would like to thank the two anonymous reviewers for their critical
1154 comments that helped improve this manuscript. Authors would also like to thank Blanca
1155 Ausín for her insight on radiocarbon dating and Serge Heussner for the retrieval of the
1156 sediment trap collected within the French MOOSE program (Mediterranean Ocean
1157 Observing System for the Environment) coordinated by CNRS-INSU and the Research
1158 Infrastructure ILICO (CNRS-IFREMER). This study was funded by the Spanish "Ministerio
1159 de Ciencia e Innovación" through a grant number PRE2019-089091 and through the project
1160 RTI2018-099489-B-100; PID2021-128322NB-I00.

1161 ## References

1162 Aldridge, D., Beer, C. J., and Purdie, D. A.: Calcification in the planktonic foraminifera;
1163   *Globigerina bulloides*; linked to phosphate concentrations in surface waters of the North
1164   Atlantic Ocean, Biogeosciences, 9, 1725–1739, https://doi.org/10.5194/bg-9-1725-2012,
1165   2012.
1166 Álvarez, M., Sanleón-Bartolomé, H., Tanhua, T., Mintrop, L., Luchetta, A., Cantoni, C.,
1167   Schroeder, K., and Civitarese, G.: The CO_2; system in the Mediterranean Sea: a basin wide
1168   perspective, Ocean Sci., 10, 69–92, https://doi.org/10.5194/os-10-69-2014, 2014.

Azibeiro, L. A., Kučera, M., Jonkers, L., Cloke-Hayes, A., and Sierro, F. J.: Nutrients and hydrography explain the composition of recent Mediterranean planktonic foraminiferal assemblages, Marine Micropaleontology, 179, 102201, https://doi.org/10.1016/j.marmicro.2022.102201, 2023.

Barker, S. and Elderfield, H.: Foraminiferal Calcification Response to Glacial-Interglacial Changes in Atmospheric CO_2, Science, 297, 833–836, https://doi.org/10.1126/science.1072815, 2002.

Bé, A. W. H., Hutson, W. H., and Be, A. W. H.: Ecology of Planktonic Foraminifera and Biogeographic Patterns of Life and Fossil Assemblages in the Indian Ocean, Micropaleontology, 23, 369, https://doi.org/10.2307/1485406, 1977.

Beaufort, L., Probert, I., and Buchet, N.: Effects of acidification and primary production on coccolith weight: Implications for carbonate transfer from the surface to the deep ocean: oceanic carbonate transfer, Geochem. Geophys. Geosyst., 8, n/a-n/a, https://doi.org/10.1029/2006GC001493, 2007.

Beer, C. J., Schiebel, R., and Wilson, P. A.: Technical Note: On methodologies for determining the size-normalised weight of planktic foraminifera, Biogeosciences, 7, 2193–2198, https://doi.org/10.5194/bg-7-2193-2010, 2010a.

Beer, C. J., Schiebel, R., and Wilson, P. A.: Testing planktic foraminiferal shell weight as a surface water $[CO_3^{2-}]$ proxy using plankton net samples, Geology, 38, 103–106, https://doi.org/10.1130/G30150.1, 2010b.

Bergamasco, A. and Malanotte-Rizzoli, P.: The circulation of the Mediterranean Sea: a historical review of experimental investigations, Advances in Oceanography and Limnology, 1, 11–28, https://doi.org/10.1080/19475721.2010.491656, 2010.

Berger, W. H.: Planktonic Foraminifera: Selective solution and the lysocline, Mar. Geol., 8, 111–138, 1970.

Bethoux, J. P., Gentili, B., Morin, P., Nicolas, E., Pierre, C., and Ruiz-Pino, D.: The Mediterranean Sea: a miniature ocean for climatic and environmental studies and a key for the climatic functioning of the North Atlantic, Progress in Oceanography, 44, 131–146, https://doi.org/10.1016/S0079-6611(99)00023-3, 1999.

Bijma, J., Hönisch, B., and Zeebe, R. E.: Impact of the ocean carbonate chemistry on living foraminiferal shell weight: Comment on "Carbonate ion concentration in glacial-age deep waters of the Caribbean Sea" by W. S. Broecker and E. Clark: COMMENT, Geochem.-Geophys.-Geosyst., 3, 1–7, https://doi.org/10.1029/2002GC000388, 2002.

Bird, C., Darling, K. F., Russell, A. D., Davis, C. V., Fehrenbacher, J., Free, A., Wyman, M., and Ngwenya, B. T.: Cyanobacterial endobionts within a major marine planktonic calcifier (*Globigerina bulloides*, Foraminifera) revealed by 16S rRNA metabarcoding, Biogeosciences, 14, 901–920, https://doi.org/10.5194/bg-14-901-2017, 2017.

Bollmann, J., Herrle, J. O., Cortés, M. Y., and Fielding, S. R.: The effect of sea water salinity on the morphology of *Emiliania huxleyi* in plankton and sediment samples, Earth and Planetary Science Letters, 284, 320–328, https://doi.org/10.1016/j.epsl.2009.05.003, 2009.

Burke, J. E., Renema, W., Henehan, M. J., Elder, L. E., Davis, C. V., Maas, A. E., Foster, G. L., Schiebel, R., and Hull, P. M.: Factors influencing test porosity in planktonic foraminifera, Biogeosciences, 15, 6607–6619, https://doi.org/10.5194/bg-15-6607-2018, 2018.

Canals, M., Puig, P., de Madron, X. D., Heussner, S., Palanques, A., and Fabres, J.: Flushing submarine canyons, Nature, 444, 354–357, https://doi.org/10.1038/nature05271, 2006.

Chapman, M. R.: Seasonal production patterns of planktonic foraminifera in the NE Atlantic Ocean: Implications for paleotemperature and hydrographic reconstructions: currents, Paleoceanography, 25, https://doi.org/10.1029/2008PA001708, 2010.

Cisneros, M., Cacho, I., Frigola, J., Canals, M., Masqué, P., Martrat, B., Casado, M., Grimalt, J. O., Pena, L. D., Margaritelli, G., and Lirer, F.: Sea surface temperature variability in the

central-western Mediterranean Sea during the last 2700 years: a multi-proxy and multi-record approach, Clim. Past, 12, 849–869, https://doi.org/10.5194/cp-12-849-2016, 2016.

Cléroux, C., Lynch-Stieglitz, J., Schmidt, M. W., Cortijo, E., and Duplessy, J.-C.: Evidence for calcification depth change of *Globorotalia truncatulinoides* between deglaciation and Holocene in the Western Atlantic Ocean, Marine Micropaleontology, 73, 57–61, https://doi.org/10.1016/j.marmicro.2009.07.001, 2009.

Coppola L., Diamond Riquier E.: MOOSE (DYFAMED), https://doi.org/10.18142/131, 2008.

Coppola, L., Raimbault, P., Mortier, L., and Testor, P. Monitoring the environment in the northwestern Mediterranean Sea, *Eos, 100,* https://doi.org/10.1029/2019EO125951, 2019.

Coppola L., Diamond Riquier E. Carval T., Dyfamed observatory data. https://doi.org/10.17882/43749, 2021.

Davis, C. V., Rivest, E. B., Hill, T. M., Gaylord, B., Russell, A. D., and Sanford, E.: Ocean acidification compromises a planktic calcifier with implications for global carbon cycling, Sci Rep, 7, 2225, https://doi.org/10.1038/s41598-017-01530-9, 2017.

Dickson, A. G.: Standard potential of the reaction: AgCl(s) +iH,(g) = Ag(s) + HCl(aq), and and the standard acidity constant of the ion HSOh in synthetic sea water from 273.15 to 318.15 K, J. Chem. Thermodyn.,22,113-127, 1990.

Dickson, A. G. and Millero, F. J.: A comparison of the equilibrium constants for the dissociation of carbonic acid in seawater media, Deep-Sea Res., 34, 1733–1743, 1987.

Dolman, A. M., Groeneveld, J., Mollenhauer, G., Ho, S. L., and Laepple, T.: Estimating Bioturbation From Replicated Small-Sample Radiocarbon Ages, Paleoceanog and Paleoclimatol, 36, https://doi.org/10.1029/2020PA004142, 2021.

Doney, S. C., Fabry, V. J., Feely, R. A., and Kleypas, J. A.: Ocean Acidification: The other CO_2 Problem, Annu. Rev. Mar. Sci., 1, 169–192, https://doi.org/10.1146/annurev.marine.010908.163834, 2009.

Durrieu de Madron, X., Zervakis, V., Theocharis, A., and Georgopoulos, D.: Comments on "Cascades of dense water around the world ocean," Progress in Oceanography, 64, 83–90, https://doi.org/10.1016/j.pocean.2004.08.004, 2005.

Durrieu de Madron, X., Houpert, L., Puig, P., Sanchez-Vidal, A., Testor, P., Bosse, A., Estournel, C., Somot, S., Bourrin, F., Bouin, M. N., Beauverger, M., Beguery, L., Calafat, A., Canals, M., Cassou, C., Coppola, L., Dausse, D., D'Ortenzio, F., Font, J., Heussner, S., Kunesch, S., Lefevre, D., Le Goff, H., Martín, J., Mortier, L., Palanques, A., and Raimbault, P.: Interaction of dense shelf water cascading and open-sea convection in the northwestern Mediterranean during winter 2012: shelf cascading and open-sea convection, Geophys. Res. Lett., 40, 1379–1385, https://doi.org/10.1002/grl.50331, 2013.

Durrieu de Madron, X., Ramondenc, S., Berline, L., Houpert, L., Bosse, A., Martini, S., Guidi, L., Conan, P., Curtil, C., Delsaut, N., Kunesch, S., Ghiglione, J. F., Marsaleix, P., Pujo-Pay, M., Séverin, T., Testor, P., Tamburini, C., and the ANTARES collaboration: Deep sediment resuspension and thick nepheloid layer generation by open-ocean convection: BNL generation by open-ocean convection, J. Geophys. Res. Oceans, 122, 2291–2318, https://doi.org/10.1002/2016JC012062, 2017.

Estrada, M., Marrasé, C., Latasa, M., Berdalet, E., Delgado, M., and Riera, T.: Variability of deep chlorophyll maximum characteristics in the Northwestern Mediterranean, Mar. Ecol. Prog. Ser., 92, 289–300, https://doi.org/10.3354/meps092289, 1993.

Figuerola, B., Hancock, A. M., Bax, N., Cummings, V. J., Downey, R., Griffiths, H. J., Smith, J., and Stark, J. S.: A Review and Meta-Analysis of Potential Impacts of Ocean Acidification on Marine Calcifiers From the Southern Ocean, Front. Mar. Sci., 8, 584445, https://doi.org/10.3389/fmars.2021.584445, 2021.

Fox, L., Stukins, S., Hill, T., and Miller, C. G.: Quantifying the Effect of Anthropogenic Climate Change on Calcifying Plankton, Sci Rep, 10, 1620, https://doi.org/10.1038/s41598-020-58501-w, 2020.

Hassoun, A. E. R., Gemayel, E., Krasakopoulou, E., Goyet, C., Abboud-Abi Saab, M., Guglielmi, V., Touratier, F., and Falco, C.: Acidification of the Mediterranean Sea from anthropogenic carbon penetration, Deep Sea Research Part I: Oceanographic Research Papers, 102, 1–15, https://doi.org/10.1016/j.dsr.2015.04.005, 2015.

Hassoun, A. E. R., Bantelman, A., Canu, D., Comeau, S., Galdies, C., Gattuso, J.-P., Giani, M., Grelaud, M., Hendriks, I. E., Ibello, V., Idrissi, M., Krasakopoulou, E., Shaltout, N., Solidoro, C., Swarzenski, P. W., and Ziveri, P.: Ocean acidification research in the Mediterranean Sea: Status, trends and next steps, Front. Mar. Sci., 9, 892670, https://doi.org/10.3389/fmars.2022.892670, 2022.

Head, M. J., Zalasiewicz, J. A., Waters, C. N., Turner, S. D., Williams, M., Barnosky, A. D., Steffen, W., Wagreich, M., Haff, P. K., Syvitski, J., Leinfelder, R., McCarthy, F. M. G., Rose, N. L., Wing, S. L., An, Z., Cearreta, A., Cundy, A. B., Fairchild, I. J., Han, Y., Sul, J. A. I. do, Jeandel, C., McNeill, J. R., and Summerhayes, C. P.: The Anthropocene is a prospective epoch/series, not a geological event, Episodes, https://doi.org/10.18814/epiiugs/2022/022025, 2022a.

Head, M. J., Steffen, W., Fagerlind, D., Waters, C. N., Poirier, C., Syvitski, J., Zalasiewicz, J. A., Barnosky, A. D., Cearreta, A., Jeandel, C., Leinfelder, R., McNeill, J. R., Rose, N. L., Summerhayes, C., Wagreich, M., and Zinke, J.: The Great Acceleration is real and provides a quantitative basis for the proposed Anthropocene Series/Epoch, Episodes, 45, 359–376, https://doi.org/10.18814/epiiugs/2021/021031, 2022b.

Heaton, T. J., Köhler, P., Butzin, M., Bard, E., Reimer, R. W., Austin, W. E. N., Bronk Ramsey, C., Grootes, P. M., Hughen, K. A., Kromer, B., Reimer, P. J., Adkins, J., Burke, A., Cook, M. S., Olsen, J., and Skinner, L. C.: Marine20—The Marine Radiocarbon Age Calibration Curve (0–55,000 cal BP), Radiocarbon, 62, 779–820, https://doi.org/10.1017/RDC.2020.68, 2020.

Hemleben, C., Spindler, M., and Anderson, O. R.: Modern Planktonic Foraminifera, 1989.

Heussner, S., Durrieu de Madron, X., Calafat, A., Canals, M., Carbonne, J., Delsaut, N., and Saragoni, G.: Spatial and temporal variability of downward particle fluxes on a continental slope: Lessons from an 8-yr experiment in the Gulf of Lions (NW Mediterranean), Marine Geology, 234, 63–92, https://doi.org/10.1016/j.margeo.2006.09.003, 2006.

Houpert, L., Durrieu de Madron, X., Testor, P., Bosse, A., D'Ortenzio, F., Bouin, M. N., Dausse, D., Le Goff, H., Kunesch, S., Labaste, M., Coppola, L., Mortier, L., and Raimbault, P.: Observations of open-ocean deep convection in the northwestern Mediterranean Sea: Seasonal and interannual variability of mixing and deep water masses for the 2007-2013 Period: deep convection obs. NWMED 2007-2013, J. Geophys. Res. Oceans, 121, 8139–8171, https://doi.org/10.1002/2016JC011857, 2016.

Ipcc: The Ocean and Cryosphere in a Changing Climate: Special Report of the Intergovernmental Panel on Climate Change, 1st ed., Cambridge University Press, https://doi.org/10.1017/9781009157964, 2022.

Jonkers, L., Hillebrand, H., and Kucera, M.: Global change drives modern plankton communities away from the pre-industrial state, Nature, 570, 372–375, https://doi.org/10.1038/s41586-019-1230-3, 2019.

Kiss, P., Jonkers, L., Hudáčková, N., Reuter, R. T., Donner, B., Fischer, G., and Kucera, M.: Determinants of Planktonic Foraminifera Calcite Flux: Implications for the Prediction of Intra- and Inter-Annual Pelagic Carbonate Budgets, Global Biogeochem Cycles, 35, https://doi.org/10.1029/2020GB006748, 2021.

Kroeker, K. J., Kordas, R. L., Crim, R., Hendriks, I. E., Ramajo, L., Singh, G. S., Duarte, C. M., and Gattuso, J.: Impacts of ocean acidification on marine organisms: quantifying sensitivities and interaction with warming, Glob Change Biol, 19, 1884–1896, https://doi.org/10.1111/gcb.12179, 2013.

Kuroyanagi, A. and Kawahata, H.: Vertical distribution of living planktonic foraminifera in the seas around Japan, Marine Micropaleontology, 53, 173–196, https://doi.org/10.1016/j.marmicro.2004.06.001, 2004.

LeGrande, A. N., Lynch-Stieglitz, J., and Farmer, E. C.: Oxygen isotopic composition of *Globorotalia truncatulinoides* as a proxy for intermediate depth density: $\delta^{18}O$ *Truncatulinoides* as proxy for mid-depth density, Paleoceanography, 19, n/a-n/a, https://doi.org/10.1029/2004PA001045, 2004.

Lirer, F., Sprovieri, M., Vallefuoco, M., Ferraro, L., Pelosi, N., Giordano, L., and Capotondi, L.: Planktonic foraminifera as bio-indicators for monitoring the climatic changes that have occurred over the past 2000 years in the southeastern Tyrrhenian Sea, Integrative Zoology, 9, 542–554, https://doi.org/10.1111/1749-4877.12083, 2014.

Lohmann, G. P. and Schweitzer, P. N.: *Globorotalia truncatulinoides'* Growth and chemistry as probes of the past thermocline: 1. Shell size, Paleoceanography, 5, 55–75, https://doi.org/10.1029/PA005i001p00055, 1990.

Lombard, F., Erez, J., Michel, E., and Labeyrie, L.: Temperature effect on respiration and photosynthesis of the symbiont-bearing planktonic foraminifera *Globigerinoides ruber*, *Orbulina universa*, and *Globigerinella siphonifera*, Limnol. Oceanogr., 54, 210–218, https://doi.org/10.4319/lo.2009.54.1.0210, 2009.

Lombard, F., da Rocha, R. E., Bijma, J., and Gattuso, J.-P.: Effect of carbonate ion concentration and irradiance on calcification in planktonic foraminifera, Biogeosciences, 7, 247–255, https://doi.org/10.5194/bg-7-247-2010, 2010.

Lombard, F., Labeyrie, L., Michel, E., Bopp, L., Cortijo, E., Retailleau, S., Howa, H., and Jorissen, F.: Modelling planktic foraminifer growth and distribution using an ecophysiological multi-species approach, Biogeosciences, 8, 853–873, https://doi.org/10.5194/bg-8-853-2011, 2011.

Loulergue, L., Parrenin, F., and Blunier, T.: New constraints on the gas age-ice age difference along the EPICA ice cores, 0–50 kyr, Clim. Past, 14, 2007.

Lüthi, D., Le Floch, M., Bereiter, B., Blunier, T., Barnola, J.-M., Siegenthaler, U., Raynaud, D., Jouzel, J., Fischer, H., Kawamura, K., and Stocker, T. F.: High-resolution carbon dioxide concentration record 650,000–800,000 years before present, Nature, 453, 379–382, https://doi.org/10.1038/nature06949, 2008.

Margaritelli, G.: *Globorotalia truncatulinoides* in Central - Western Mediterranean Sea during the Little Ice Age, Marine Micropaleontology, 11, 2020.

Margaritelli, G., Lirer, F., Schroeder, K., Cloke-Hayes, A., Caruso, A., Capotondi, L., Broggy, T., Cacho, I., and Sierro, F. J.: *Globorotalia truncatulinoides* in the Mediterranean Basin during the Middle–Late Holocene: Bio-Chronological and Oceanographic Indicator, Geosciences, 12, 244, https://doi.org/10.3390/geosciences12060244, 2022.

Marshall, B. J., Thunell, R. C., Henehan, M. J., Astor, Y., and Wejnert, K. E.: Planktonic foraminiferal area density as a proxy for carbonate ion concentration: A calibration study using the Cariaco Basin ocean time series: foraminiferal area density [CO_3^{2-}] PROXY, Paleoceanography, 28, 363–376, https://doi.org/10.1002/palo.20034, 2013.

Marty, J.-C., Chiavérini, J., Pizay, M.-D., and Avril, B.: Seasonal and interannual dynamics of nutrients and phytoplankton pigments in the western Mediterranean Sea at the DYFAMED time-series station (1991–1999), Deep Sea Research Part II: Topical Studies in Oceanography, 49, 1965–1985, https://doi.org/10.1016/S0967-0645(02)00022-X, 2002.

Mehrbach, C., Culberson, C. H., Hawley, J. E., and Pytkowicx, R. M.: measurement of the apparent dissociation constants of carbonic acid in seawater at atmospheric pressure, Limnol. Oceanogr., 18, 897–907, https://doi.org/10.4319/lo.1973.18.6.0897, 1973.

Meier, K. J. S., Beaufort, L., Heussner, S., Ziveri, P., and Université, A.-M.: The role of ocean acidification in *Emiliania huxleyi* coccolith thinning in the Mediterranean Sea, 13, 2014.

Millot, C.: The Gulf of Lions' hydrodynamics, Continental Shelf Research, 10, 885–894, https://doi.org/10.1016/0278-4343(90)90065-T, 1990.

de Moel, H., Ganssen, G. M., Peeters, F. J. C., Jung, S. J. A., Kroon, D., Brummer, G. J. A., and Zeebe, R. E.: Planktic foraminiferal shell thinning in the Arabian Sea due to anthropogenic ocean acidification?, 9, 2009.

Monaco, A., de Madron, X. D., Radakovitch, O., Heussner, S., and Carbonne, J.: Origin and variability of downward biogeochemical #uxes on the Rhone continental margin (NW mediterranean), 29, 1999.

Moy, A. D., Howard, W. R., Bray, S. G., and Trull, T. W.: Reduced calcification in modern Southern Ocean planktonic foraminifera, Nature Geosci, 2, 276–280, https://doi.org/10.1038/ngeo460, 2009.

Nguyen, T. M. P., Petrizzo, M. R., and Speijer, R. P.: Experimental dissolution of a fossil foraminiferal assemblage (Paleocene–Eocene Thermal Maximum, Dababiya, Egypt): Implications for paleoenvironmental reconstructions, Marine Micropaleontology, 73, 241–258, https://doi.org/10.1016/j.marmicro.2009.10.005, 2009.

Orr, J. C., Fabry, V. J., Aumont, O., Bopp, L., Doney, S. C., Feely, R. A., Gnanadesikan, A., Gruber, N., Ishida, A., Joos, F., Key, R. M., Lindsay, K., Maier-Reimer, E., Matear, R., Monfray, P., Mouchet, A., Najjar, R. G., Plattner, G.-K., Rodgers, K. B., Sabine, C. L., Sarmiento, J. L., Schlitzer, R., Slater, R. D., Totterdell, I. J., Weirig, M.-F., Yamanaka, Y., and Yool, A.: Anthropogenic ocean acidification over the twenty-first century and its impact on calcifying organisms, Nature, 437, 681–686, https://doi.org/10.1038/nature04095, 2005.

Osborne, E. B., Thunell, R. C., Marshall, B. J., Holm, J. A., Tappa, E. J., Benitez-Nelson, C., Cai, W., and Chen, B.: Calcification of the planktonic foraminifera *Globigerina bulloides* and carbonate ion concentration: Results from the Santa Barbara Basin, Paleoceanography, 31, 1083–1102, https://doi.org/10.1002/2016PA002933, 2016.

Pallacks, S., Anglada-Ortiz, G., Belen Martrat, P. Graham Mortyn, Grelaud, M., Incarbona, A., Schiebel, R., Garcia-Orellana, J., and Ziveri, P.: Western Mediterranean marine cores show that foraminiferal mass and flux are being influenced by enhanced anthropogenic pressure, https://doi.org/10.13140/RG.2.2.26245.99045, 2020a.

Pallacks, S., Anglada-Ortiz, G., Belen Martrat, P Graham Mortyn, Grelaud, M., Incarbona, A., Schiebel, R., Garcia-Orellana, J., and Ziveri, P.: Western Mediterranean marine cores show that foraminiferal test calcite mass is being influenced by enhanced anthropogenic pressure, https://doi.org/10.13140/RG.2.2.34091.57124, 2020b.

Parrenin, F., Jouzel, J., Kawamura, K., Lemieux-Dudon, B., Loulergue, L., Masson-Delmotte, V., Narcisi, B., Raisbeck, G., Raynaud, D., Ruth, U., Schwander, J., Severi, M., Spahni, R., Steffensen, J. P., Svensson, A., Udisti, R., Waelbroeck, C., and Wolff, E.: The EDC3 chronology for the EPICA Dome C ice core, Clim. Past, 13, 2007.

Pujol, C. and Grazzini, C. V.: Distribution patterns of live planktic foraminifers as related to regional hydrography and productive systems of the Mediterranean Sea, Marine Micropaleontology, 25, 187–217, https://doi.org/10.1016/0377-8398(95)00002-I, 1995.

Rebotim, A., Voelker, A. H. L., Jonkers, L., Waniek, J. J., Meggers, H., Schiebel, R., Fraile, I., Schulz, M., and Kucera, M.: Factors controlling the depth habitat of planktonic foraminifera in the subtropical eastern North Atlantic, Biogeosciences, 14, 827–859, https://doi.org/10.5194/bg-14-827-2017, 2017.

Reimer, P. J. and Reimer, R. W.: A Marine Reservoir Correction Database and On-Line Interface, Radiocarbon, 43, 461–463, https://doi.org/10.1017/S0033822200038339, 2001.

Rigual-Hernández, A. S., Sierro, F. J., Bárcena, M. A., Flores, J. A., and Heussner, S.: Seasonal and interannual changes of planktic foraminiferal fluxes in the Gulf of Lions (NW Mediterranean) and their implications for paleoceanographic studies: Two 12-year sediment trap records, Deep Sea Research Part I: Oceanographic Research Papers, 66, 26–40, https://doi.org/10.1016/j.dsr.2012.03.011, 2012.

Sabine, C. L., Feely, R. A., Gruber, N., Key, R. M., Lee, K., Bullister, J. L., Wanninkhof, R., Wong, C. S., Wallace, D. W. R., Tilbrook, B., Millero, F. J., Peng, T.-H., Kozyr, A., Ono, T., and Rios, A. F.: The Oceanic Sink for Anthropogenic CO_2, Science, 305, 367–371, https://doi.org/10.1126/science.1097403, 2004.

Schiebel, R.: Planktic foraminiferal sedimentation and the marine calcite budget: marine calcite budget, Global Biogeochem. Cycles, 16, 3-1-3–21, https://doi.org/10.1029/2001GB001459, 2002.

Schiebel, R., Waniek, J., Bork, M., and Hemleben, C.: Planktic foraminiferal production stimulated by chlorophyll redistribution and entrainment of nutrients, Deep Sea Research Part I: Oceanographic Research Papers, 48, 721–740, https://doi.org/10.1016/S0967-0637(00)00065-0, 2001.

Schiebel, R. and Hemleben, C.: Interannual variability of planktic foraminiferal populations and test flux in the eastern North Atlantic Ocean (JGOFS), 44, 2000.

Schiebel, R. and Hemleben, C.: Planktic Foraminifers in the Modern Ocean, Springer Berlin Heidelberg, Berlin, Heidelberg, https://doi.org/10.1007/978-3-662-50297-6, 2017.

Schiebel, R. and Hemleben, Ch.: Modern planktic foraminifera, Palaeont. Z., 79, 135–148, 2005.

Schiebel, R., Waniek, J., Zeltner, A., and Alves, M.: Impact of the Azores Front on the distribution of planktic foraminifers, shelled gastropods, and coccolithophorids, Deep Sea Research Part II: Topical Studies in Oceanography, 49, 4035–4050, https://doi.org/10.1016/S0967-0645(02)00141-8, 2002.

Schneider, A., Wallace, D. W. R., and Körtzinger, A.: Alkalinity of the Mediterranean Sea: alkalinity of the mediterranean sea, Geophys. Res. Lett., 34, https://doi.org/10.1029/2006GL028842, 2007.

Stuiver, M. and Braziunas, T. F.: Modeling Atmospheric [14]C Influences and [14]C Ages of Marine Samples to 10,000 BC, Radiocarbon, 35, 137–189, https://doi.org/10.1017/S0033822200013874, 1993.

Stuiver, M. and Reimer, P. J.: Extended [14]C Data Base and Revised CALIB 3.0 [14]C Age Calibration Program, Radiocarbon, 35, 215–230, https://doi.org/10.1017/S0033822200013904, 1993.

Takagi, H., Kimoto, K., Fujiki, T., Saito, H., Schmidt, C., Kucera, M., and Moriya, K.: Characterizing photosymbiosis in modern planktonic foraminifera, Biogeosciences, 16, 3377–3396, https://doi.org/10.5194/bg-16-3377-2019, 2019.

Touratier, F., Guglielmi, V., Goyet, C., Prieur, L., Pujo-Pay, M., Conan, P., and Falco, C.: Distributions of the carbonate system properties, anthropogenic CO_2 and acidification during the 2008 BOUM cruise (Mediterranean Sea), Biogeochemistry: Open Ocean, https://doi.org/10.5194/bgd-9-2709-2012, 2012.

de Villiers, S.: Optimum growth conditions as opposed to calcite saturation as a control on the calcification rate and shell-weight of marine foraminifera, Marine Biology, 144, 45–49, https://doi.org/10.1007/s00227-003-1183-8, 2004.

Weinkauf, M. F. G., Kunze, J. G., Waniek, J. J., and Kučera, M.: Seasonal Variation in Shell Calcification of Planktonic Foraminifera in the NE Atlantic Reveals Species-Specific Response to Temperature, Productivity, and Optimum Growth Conditions, PLoS ONE, 11, e0148363, https://doi.org/10.1371/journal.pone.0148363, 2016

Wilke, I., Meggers, H., and Bickert, T.: Depth habitats and seasonal distributions of recent planktic foraminifers in the Canary Islands region (29°N) based on oxygen isotopes, Deep Sea Research Part I: Oceanographic Research Papers, 56, 89–106, https://doi.org/10.1016/j.dsr.2008.08.001, 2009.

Zarkogiannis, S. D., Iwasaki, S., Rae, J. W. B., Schmidt, M. W., Mortyn, P. G., Kontakiotis, G., Hertzberg, J. E., and Rickaby, R. E. M.: Calcification, Dissolution and Test Properties

1471   of Modern Planktonic Foraminifera From the Central Atlantic Ocean, Front. Mar. Sci., 9,
1472   864801, https://doi.org/10.3389/fmars.2022.864801, 2022.
1473